

# Verification of First-Order Methods for Parametric Quadratic Optimization

Vinit Ranjan      Bartolomeo Stellato

Department of Operations Research and Financial Engineering  
Princeton University

March 7, 2024

## Abstract

We introduce a numerical framework to verify the finite step convergence of first-order methods for parametric convex quadratic optimization. We formulate the verification problem as a mathematical optimization problem where we maximize a performance metric (*e.g.*, fixed-point residual at the last iteration) subject to constraints representing proximal algorithm steps (*e.g.*, linear system solutions, projections, or gradient steps). Our framework is highly modular because we encode a wide range of proximal algorithms as variations of two primitive steps: affine steps and element-wise maximum steps. Compared to standard convergence analysis and performance estimation techniques, we can explicitly quantify the effects of warm-starting by directly representing the sets where the initial iterates and parameters live. We show that the verification problem is  $\mathcal{NP}$ -hard, and we construct strong semidefinite programming relaxations using various constraint tightening techniques. Numerical examples in non-negative least squares, network utility maximization, Lasso, and optimal control show a significant reduction in pessimism of our framework compared to standard worst-case convergence analysis techniques.

## 1 Introduction

### 1.1 Parametric quadratic programs

We consider convex [quadratic programs \(QPs\)](#) of the form

$$\begin{aligned} & \text{minimize} && (1/2)x^T P x + q(\theta)^T x \\ & \text{subject to} && A x \in \mathcal{C}(\theta), \end{aligned} \tag{1}$$

with decision variable  $x \in \mathbf{R}^n$ . In this work, we focus on the setting where we solve several instances of (1) where only parameters  $\theta \in \Theta \subset \mathbf{R}^p$  vary. The objective is defined by a symmetric positive semidefinite matrix  $P \in \mathbf{S}_+^{n \times n}$  and a linear term  $q(\theta) \in \mathbf{R}^n$  that depends on parameter  $\theta$ . The constraints are defined by a matrix  $A \in \mathbf{R}^{m \times n}$ , and a nonempty, closed, convex set  $\mathcal{C}(\theta) \subseteq \mathbf{R}^n$  that depends on  $\theta$ . In this paper, the set  $\mathcal{C}(\theta)$  takes the form

$$\mathcal{C}(\theta) = [l(\theta), u(\theta)] = \{v \in \mathbf{R}^m \mid l_i(\theta) \leq v_i \leq u_i(\theta)\},$$

with  $l_i(\theta) \in \{-\infty\} \cup \mathbf{R}$  and  $u_i(\theta) \in \{\infty\} \cup \mathbf{R}$  for all  $\theta \in \Theta$ . We encode equality constraints in this form by setting  $l_i(\theta) = u_i(\theta)$  for all  $\theta \in \Theta$ . We refer to problem (1) as a (*convex*) *parametric quadratic program (PQP)*.

**Applications.** A huge variety of applications from finance, engineering, operations research, and other fields involve the solution of parametric problems of the form (1). Financial applications include portfolio optimization, where we seek to rebalance asset allocation where parameters correspond to new returns estimates [Mar52, BMOW14]. Applications in machine learning include hyperparameter tuning in *support vector machines (SVMs)* [CV95], Lasso [Tib96, CWB07] and Huber fitting [Hub64]. Several problems in signal processing are also of the form (1), where the parameters are the measured signals [MB10b]. Also in control engineering, *model predictive control (MPC)* problems involve the solution of PQPs in real-time [BBM17, RM09, MT21].

**Solution algorithm.** Our goal is to solve problem (1) using *first-order methods* of the form

$$z^{k+1} = T_\theta(z^k), \quad k = 0, 1, \dots, \quad (2)$$

where  $T_\theta$  is a *fixed-point operator* that depends on the parameter  $\theta$ , and  $z^k \in \mathbf{R}^d$  is the iterate at iteration  $k$ . The *fixed-points*  $z^* = T_\theta(z^*)$  correspond to the optimal solutions of (1). To measure the distance to optimality, we define the *fixed-point residual* evaluated at  $z^k$  as  $T_\theta(z^k) - z^k$ , and measure its magnitude  $\|T_\theta(z^k) - z^k\|$ . As  $k \rightarrow \infty$ , the fixed-point residual converges to 0 in well-known cases (*e.g.*, averaged [BC17, Cor. 5.8] or contractive [BC17, Thm. 1.50] [RY22, Thm. 2.4.2] operators). In this paper, we study the behavior of the fixed-point operator  $T_\theta$  without making any convergence assumption.

**Verification problem.** In several applications, we can only afford a specific number of iterations of algorithm (2) to compute an optimal solution for each instance of problem (1) in real-time [BBM17, MB10b]. In this work, we numerically verify that the first-order method (2) is able to compute an approximate solution in  $K$  iterations for any instance of problem (1), by checking the condition

$$\|T_\theta^K(z^0) - T_\theta^{K-1}(z^0)\|^2 \leq \epsilon, \quad \forall z^0 \in Z, \quad \forall \theta \in \Theta, \quad (3)$$

where  $\epsilon > 0$  is our tolerance and  $T_\theta^K$  is the  $K$ -times composition of operator  $T_\theta$ . We represent the set of initial iterates as  $Z \subset \mathbf{R}^d$  (for cold-started algorithms,  $Z = \{0\}$ ). In this paper, we derive exact formulations and tractable approximations for this problem, highlighting its benefits compared to classical worst-case complexity verification techniques.

## 1.2 Related work

**First-order methods.** First-order optimization methods rely only on first-order derivative information [Bec17] and they were first applied to solve QPs in the 1950s [FW56]. Operator splitting algorithms [BC17], such as proximal algorithms [PB13] and the alternating direction method of multipliers (ADMM) [GM76, DR56, BPC<sup>+</sup>11], are a particular class of first-order methods which solve an optimization problem by breaking it into simpler components (operators). Recently, first-order methods have gained wide popularity in parametric optimization and real-time applications for two reasons. First, they involve computationally cheap iterations that are ideal for embedded processors with limited computing resources, such as those found in embedded control systems [JGR<sup>+</sup>14, OSB13, SSS<sup>+</sup>16]. Second, they can be easily warm-started, which greatly reduces the real-time computational cost. For these reasons, several general-purpose first-order optimization solvers are now available, including PDLP [ADH<sup>+</sup>21] for linear programs (LPs), SCS [OCPB16] for semidefinite programs (SDPs), and the OSQP solver [SBG<sup>+</sup>20] for QPs. Despite the latest advances, first-order methods are still highly sensitive to data and can exhibit very slow convergence for badly scaled problems, which can be dangerous for safety-critical applications. In this project, given a family of PQPs, we will directly verify the performance of a specific first-order method for a fixed-number of iterations, while taking into account the effects of parameter variations and warm-starting.

**Classical convergence analysis.** Classical convergence analysis techniques for first-order methods in convex optimization consider general classes of problems, such as minimization of smooth or strongly convex functions [Nes18, Chapter 2][Bec17, Chapter 5]. Some of these tools rely on operator theory by modeling the optimization problem in terms of finding a zero of the sum of monotone operators [RY22]. The monotonicity property is particularly general, *e.g.*, the subdifferential of any convex proper function is a monotone operator [RY22, Section 2.2]. While often tight, these results can be quite pessimistic in the context considered in this work. First, they focus on generic classes of problems without targeting the structure of PQPs. For example, in several applications such as linear MPC or Lasso, the PQPs in equation (1) have a constant quadratic term, while other linear terms vary [SBG<sup>+</sup>20]. However, while all problems in a specific family have the same smoothness constant, first-order algorithms can exhibit very different practical performance. In fact, they can often converge more quickly than worst-case bounds [RJM12, Section VII] [SBG<sup>+</sup>20]. Second, classical convergence analysis techniques focus on asymptotic rates of convergence, which are particularly suited for a large number of algorithm steps, *i.e.*,  $K \rightarrow \infty$ . However, in real-time applications we have a finite budget of iterations which we cannot exceed. Compared to classical convergence analysis, this paper focuses on verifying that a first-order method provably achieves a high-quality solution for a specific family of PQPs, within a fixed number of iterations.

**Computer-assisted convergence analysis.** There are two primary approaches to automate the analysis of first-order methods for convex optimization, the *performance estimation*

*problem (PEP)* approach, and the *integral quadratic constraints (IQCs)* approach. The PEP approach finds the worst-case finite sequence of iterates and problem instance to compute a performance guarantee for a given first-order method [DT14, THG17c, THG17a]. Thanks to the easy-to-use PESTO [THG17b] and PEPit [GMG+22] toolboxes, PEP has led to many results in operator splitting algorithms [THG17a, RTBG20], distributed optimization [CH23] and the specific case of quadratic functions [BHG22, BHG23]. The IQC approach, instead, interprets the optimization algorithm as a dynamical system [LRP16, TVSL18, HL17] and builds sufficient conditions for convergence (stability) via integral quadratic constraints. Both PEP and IQC approaches solve a SDP to compute the worst-case bounds. In particular, PEP provides guarantees for a finite number of steps, while the IQC approach provides infinite-horizon bounds by solving a smaller problem that is independent from the number of steps considered. In addition, the IQC approach can only analyze linearly convergent algorithms, while the PEP approach can deal with sublinearly convergent methods. The PEP approach has been extended to a nonconvex formulation that can be used to generate theoretically optimal first order methods via custom branch-and-bound procedures [DGVPR23, JDGR23]. In this work, we also solve SDPs to analyze the performance of first-order methods for a finite number of steps, but we focus on the geometric properties of the iterates for a specific parametric family of problems. In Section 3, we highlight the differences between our framework and PEP, explaining the main advantages and disadvantages.

**Neural network verification.** Our work draws inspiration from neural network verification techniques, which aim to certify that a trained network produces the correct output for any acceptable input (*e.g.*, perturbation of the training data) [Alb21]. These approaches formulate verification as an optimization problem where the objective encodes the performance quality (*e.g.*, distance between network output and classification threshold) while the constraints represent the input propagation across the network layers. Solving such problems can be interpreted as searching for adversarial examples that challenge the network behavior. Several recent techniques address this problem by either global optimization tools, heuristics, or convex relaxations [LAL+21]. Global techniques (also called, complete verifiers) encode the verification problem as a mixed-integer linear program (MILP) [FJ18, TXT19, BLT+20] where the discrete decisions correspond to identifying specific regions of piecewise (*e.g.*, ReLU) activation functions. Thanks to recent developments in efficient bound propagation [ZWC+18, WZX+21], custom cutting planes [ZWX+22a], and GPU-based bound tightening [XZW+21] and branch-and-bound algorithm [ZWX+22b], global optimization techniques were able to scale to large neural networks. However, all such algorithms ultimately rely on exhaustive search which can be computationally challenging. Several relaxed formulations seek to overcome this challenge using linear programming [DDK+20, CWKF22], and semidefinite programming [FMP22, BSAP22, RSL18, NP21]. By analyzing finite step algorithms as fixed-depth computational graphs, our approach is closely related to neural network verification. In a very similar spirit, we search for worst-case inputs of our algorithm (*i.e.*, problem parameters and initial iterates) to verify that a convergence criterion is within the desired threshold. In particular, we show that several operators in neural network

graphs, such as ReLU activation functions and feedforward linear transformation, correspond to steps of proximal operators for solving QPs.

**Generalization bounds in learned optimizers.** Popular machine learning approaches, such a *learning to optimize (L2O)* [CCC<sup>+</sup>22] or *amortized optimization* [Amo23], seek to improve the performance of optimization algorithms by learning algorithm steps for a specific distribution of problem instances. Unfortunately, verifying the performance of such learned algorithms is still an open challenge. By considering  $K$  steps of a first-order method as a computational graph, Sambharya et al. [SHAS22, SHAS23] combine PAC-Bayes [McA98, STW97] and monotone operator [BC17] theories to provide probabilistic generalization bounds on the fixed-point residual. While also analyzing optimization algorithms as fixed-depth computational graphs, in this work we focus on deterministic iterations without learned components and we model the distribution of problems as a parametric family where parameters fall in a predefined convex set.

### 1.3 Contributions

In this paper, we present a framework to verify the performance of first-order methods for parametric quadratic optimization. Our contributions are as follows:

- We define a verification problem to analyze the performance of first-order methods for parametric quadratic optimization as a mathematical optimization problem. We encode a variety of proximal algorithms as combinations of two *primitive steps*: affine steps and element-wise maximum steps. We also explicitly quantify the effects of warm-starting by directly representing the sets where the initial iterates and parameters live.
- We show that for unconstrained PQPs the verification problem is a convex semidefinite program, and we provide illustrative examples to compare our formulation to the performance estimation approach. For constrained PQPs, we show that the verification problem is  $\mathcal{NP}$ -hard.
- We construct strong convex SDP relaxations for constrained PQPs based on the primitive steps and the sets where parameters and initial iterates live. We also strengthen the relaxation with various bound propagation and constraint tightening techniques.
- We compare the performance of our approach with standard convergence analysis and performance estimation tools, obtaining less pessimistic worst-case bounds in various numerical examples from nonnegative least-squares, network utility maximization, Lasso, and optimal control. We also show PQP instances where our approach can uncover details about practical convergence behavior that the standard analysis does not. The code to reproduce these results is available at [https://github.com/stellatogrp/algorithm\\_verification](https://github.com/stellatogrp/algorithm_verification).

## 2 Performance verification

From problem (3), our goal is to verify that all realizations of the parametric family lead to an iterate sequence with small fixed-point residual. This is equivalent to checking that the optimal objective of the following optimization problem is less than a threshold  $\epsilon > 0$ :

$$\begin{aligned} & \text{maximize} && \|z^K - z^{K-1}\|^2 \\ & \text{subject to} && z^{k+1} = T_\theta(z^k), \quad k = 0, \dots, K-1 \\ & && z^0 \in Z, \quad \theta \in \Theta, \end{aligned} \tag{VP}$$

with variables being the problem parameter  $\theta \in \mathbf{R}^p$  and the iterates  $z^0, \dots, z^K \in \mathbf{R}^d$ . While a fixed-point iteration can be written as a single operator  $T_\theta$ , often times  $T_\theta$  is composed of  $l$  different operators, *i.e.*,

$$z^{k+1} = T_\theta(z^k) = (S_\theta^1 \circ S_\theta^2 \circ \dots \circ S_\theta^l)(z^k). \tag{4}$$

We discuss specific choices of  $S_\theta^j$  for  $j = 1, \dots, l$  in Section 2.1 and 2.2. In the following, we simplify the notation by dropping index  $j$ , and expressing each operator as

$$y = S_\theta(x),$$

where  $x \in \mathbf{R}^d$  is its input and  $y \in \mathbf{R}^d$  its output. Lastly, we discuss the initial sets  $Z$  and the parameter sets  $\Theta$  in Section 2.3.

### 2.1 Primitive algorithm steps

We incorporate fixed-point iterations as constraints to link successive iterates. We present two fundamental operators that serve as building blocks for more complex iterations.

**Affine.** Consider the *affine* operator  $y = S_\theta(x)$  representing the solution of the following linear system

$$Dy = Ax + Bq(\theta), \tag{5}$$

where  $A$  and  $D$  are square matrices in  $\mathbf{R}^{d \times d}$  and  $B \in \mathbf{R}^{d \times n}$ . We assume that  $D$  is invertible, which makes  $y$  the unique solution to a linear system and therefore a well defined iteration. Affine steps can have varying coefficients per iteration, *i.e.*,  $A^k, B^k, D^k$  for  $k = 0, \dots, K-1$ .

**Element-wise maximum.** Consider the *element-wise maximum* of  $x$  and  $l(\theta)$ , *i.e.*,  $y = S_\theta(x) = \max\{x, l(\theta)\}$ . We can represent this operator with the following conditions [FMP22, Section III.D][BSAP22, Section 2.2]:

$$y = \max\{x, l(\theta)\} \iff y \geq l(\theta), \quad y \geq x, \quad (y - l(\theta))^T (y - x) = 0. \tag{6}$$

## 2.2 Fixed-point operators

Using the primitive steps above, we now define operators representing fixed-point algorithm steps.

**Gradient steps.** Consider a gradient step with step size  $t$  mapping iterate  $x$  to  $y$ ,

$$y = x - t\nabla f_\theta(x) = (I - tP)x - tq(\theta).$$

Here, in the second equality we used the gradient of a quadratic function  $\nabla f_\theta(x) = Px + q(\theta)$ . We can write this step as an affine step in equation (5) with  $D = I$ ,  $A = I - tP$ , and  $B = -tI$ . This formulation can also represent varying step sizes  $t_k$ , by having  $A^k = I - t_k P$  and  $B^k = -t_k I$ .

**Momentum steps.** Momentum steps such as Nesterov’s acceleration are commonly used to improve convergence of first order methods [Nes83, BT09]. We can write a Nesterov’s accelerated gradient step as the combination of two steps mapping iterates  $(r, w)$  to  $(\tilde{r}, \tilde{w})$ ,

$$\begin{aligned}\tilde{w} &= r - t\nabla f_\theta(r) \\ \tilde{r} &= (1 + \beta)\tilde{w} - \beta w.\end{aligned}$$

By substituting the gradient  $\nabla f_\theta(x) = Px + q(\theta)$ , and plugging the first step into the second one, we can write

$$\begin{aligned}\tilde{w} &= (I - tP)r - tq(\theta) \\ \tilde{r} &= -\beta w + (1 + \beta)(I - tP)r - t(1 + \beta)q(\theta).\end{aligned}$$

This step corresponds to an affine step in equation (5) with  $y = (\tilde{w}, \tilde{r})$ ,  $x = (w, r)$ , and

$$D = I, \quad A = \begin{bmatrix} 0 & I - tP \\ -\beta I & (1 + \beta)(I - tP) \end{bmatrix}, \quad B = \begin{bmatrix} -tI \\ -t(1 + \beta)I \end{bmatrix}.$$

In some variants, parameters  $\beta$  are updated at each iteration using predefined rule, *e.g.*,  $\beta^k = (k - 1)/(k - 2)$  [Nes83]. We can represent such cases in our framework by having varying matrices  $A^k$ , and  $B^k$ .

**Proximal steps.** We model several proximal steps with are the building blocks of commonly used proximal algorithms [PB13, Section 1.1]. For a function  $f : \mathbf{R}^d \rightarrow \mathbf{R}$ , the proximal operator  $\mathbf{prox}_f : \mathbf{R}^d \rightarrow \mathbf{R}^d$  is defined by:

$$y = \mathbf{prox}_f(x) = \underset{v}{\operatorname{argmin}} (f(v) + (1/2) \|v - x\|_2^2).$$

We focus on the following proximal operators, summarized in Table 1:

- **$\ell_1$ -norm.** The proximal operator of a function  $f(x) = \lambda\|x\|_1$  is the (element-wise) *soft-thresholding* operator [PB13, Section 6.5.2],

$$y = \mathbf{prox}_f(x) = (x - \lambda)_+ - (-x - \lambda)_+ = \max\{x, \lambda\} - \max\{-x, \lambda\},$$

where  $(v)_+ = \max\{v, 0\}$ . The soft-thresholding operator is, therefore, the composition of two elementwise maximum steps with an affine subtraction step.

- **Quadratic function.** The proximal operator of a convex quadratic function  $f(x) = (1/2)x^T Px + q(\theta)^T x + c$ , with  $P \in \mathbf{S}_+^n$ , is [PB13, Section 6.1.1]

$$y = \mathbf{prox}_f(x) = (I + P)^{-1}(x - q(\theta)).$$

Since positive semidefiniteness of  $P$  implies invertibility of  $I + P$ , this corresponds to an affine step with  $D = I + P$ ,  $A = I$ , and  $B = -I$ .

- **Indicator function of a box.** Consider the indicator function of a box  $C(\theta) = [l(\theta), u(\theta)]$  defined as  $f(x) = \mathcal{I}_{[l(\theta), u(\theta)]}(x) = 0$  if  $l(\theta) \leq x \leq u(\theta)$  and  $\infty$  otherwise. Its proximal operator is the projection operator [PB13, Section 1.2]

$$y = \mathbf{prox}_f(x) = \max\{\min\{x, u(\theta)\}, l(\theta)\} = \max\{-\max\{-x, -u(\theta)\}, l(\theta)\},$$

which corresponds to the composition of two element-wise maximum steps.

## 2.3 Initial iterate and parameter sets

We impose constraints on the initial iterates  $z^0 \in Z$ , and the parameters  $\theta \in \Theta$ , where  $Z$  and  $\Theta$  are convex sets of the following forms.

**Hypercubes.** We can represent hypercubes of the form  $\{v \in \mathbf{R}^d \mid l \leq v \leq u\}$ , with element-wise inequalities and  $l_i \in \{-\infty\} \cup \mathbf{R}$  and  $u_i \in \{\infty\} \cup \mathbf{R}$ .

**Polyhedra.** We represent polyhedral constraints of the form  $\{v \in \mathbf{R}^d \mid Av \leq b\}$ , with element-wise inequalities defined by  $A \in \mathbf{R}^{\ell \times d}$  and  $b \in \mathbf{R}^\ell$ .

**$\ell_p$ -balls.** For  $p = 1, 2, \infty$ , we consider  $\ell_p$  balls centered at  $c$  with radius  $r$ , that is  $\{v \in \mathbf{R}^d \mid \|v - c\|_p \leq r\}$ . We define  $\ell_1$  balls using linear inequalities and  $\ell_2$  balls with quadratic inequalities. Lastly,  $\ell_\infty$  balls are special cases of hypercubes, which we treat separately.

## 3 Differences from performance estimation problems

In this section, we highlight specific differences from the PEP framework. One attractive property of the PEP framework is its dimension-free SDPs formulations. That is, the size of the variables in a PEP SDP scales linearly in  $K$  and does not depend on the dimension

of the iterates. Our verification problem (VP), instead, is not dimension-free and is more computationally intensive to solve. However, we observe the benefits of much tighter bound analysis for PQPs. We showcase some comparison examples for unconstrained PQPs in Section 3.1.

**Functional representation.** Since the first seminal papers [DT14, THG17c], the PEP framework considers the class of  $L$ -smooth and  $\mu$ -strongly convex functions. To represent such infinite-dimensional objects using tractable SDP formulations, PEP uses *interpolation constraints* representing their effects on finite-dimensional quantities of interest (*e.g.*, gradients, functions values). Recent works derived necessary and sufficient interpolation constraints specifically designed for *homogeneous* quadratic functions [BHG22, BHG23]. However, while tighter than generic interpolation constraints, such inequalities are no longer sufficient for nonhomogeneous quadratic functions [BHG23, Section 3.4].

In this work, we consider a specific class of parametric quadratic functions where the quadratic term is constant. Rather than using interpolation inequalities, we directly represent the algorithm steps as affine steps or element-wise maximum steps. Overall, our functional representation can be seen as an explicit characterization of gradient and proximal information as opposed to the implicit characterization in PEP.

**Parametrization and functional shifts.** Consider two different PQP instances indexed by  $\theta_1$  and  $\theta_2$ , *i.e.*, and with the same matrix  $P$  but different linear terms  $q(\theta_1)$  and  $q(\theta_2)$ . Since  $P$  is the same, both PQPs have the same smoothness and strong convexity properties, so a PEP SDP can only differentiate between these two by altering the initial condition  $\|z^0 - z^*(\theta)\|^2 \leq R^2$ , where the optimal solution is  $z^*(\theta) = P^{-1}q(\theta)$ . Therefore, for a given initial iterate  $z^0$ ,  $R$  must be large enough to consider the worst-case distance  $\max\{\|z^0 - z^*(\theta_1)\|, \|z^0 - z^*(\theta_2)\|\}$ , which can lead to a large amount of conservatism. In contrast, our explicit characterization of how  $\theta$  enters into the problem allows for a tighter bound analysis.

By directly considering the function curvature, the PEP problem is invariant under any orthogonal transformation of the iterates [DT14, Section 3.1]. In addition, the classes of strongly convex and smooth functions [THG17c, Section 3] and homogeneous quadratic functions [BHG22, Section 4] are invariant under additive shifts in the domain. In this way, the optimal solution  $x^*$  can be shifted to 0 without loss of generality. While these conditions mostly serve to simplify the PEP formulation, in the practical settings considered in this work, we have access to the explicit form of  $P$  and  $q(\theta)$  as opposed to more general function classes. By dropping the dimension-free property for our verification problems, we are able to encode the specific PQP structure.

**Gram matrix and the initial set.** The PEP SDPs use a Gram matrix formulation to represent the interpolation conditions in terms of function values and inner products between iterates and gradients. However, this means when solving a PEP SDP, we optimize over the inner product values and we do not have access to the vectors themselves. So, the PEP

framework cannot express specific  $\ell_2$ -ball or box constraints to analyze warm-starting. For example, consider a constraint of the form

$$\|z^0 - v\| \leq 1 \iff (z^0)^T z^0 - 2v^T z^0 + v^T v \leq 1,$$

where  $v$  is a given vector. Since the Gram matrix can only represent inner products by their value, it cannot uniquely identify the components of vectors  $v$  and  $z^0$ . In contrast, the vector characterization in our verification problem allows to explicitly represent this kind of constraints in terms of  $v$ .

**Relative vs. absolute bounds.** The performance estimation problem is a flexible framework to compute relative convergence bounds with respect to the initial distance to optimality. Specifically, PEP computes the smallest constant  $\tau$  (*i.e.*, contraction factor) that bounds the optimality gap after  $K$  iterations using the initial distance from the optimal solution (see [GMG<sup>+</sup>22, Section 2.1]),

$$\|z^K - z^*\|^2 \leq \tau \|z^0 - z^*\|^2. \tag{7}$$

These bounds are relative because they rely on the initial distance to optimality,  $\|z^0 - z^*\|^2$ . In contrast, our method directly computes the worst-case bound without using any information on the optimal solution  $z^*$  (*e.g.*, initial distance to optimality), and, therefore, it provides absolute convergence bounds.

### 3.1 Unconstrained QP

Consider an unconstrained PQP with  $q(\theta) = \theta$  of the form

$$\text{minimize } (1/2)x^T P x + \theta^T x, \tag{8}$$

where  $P$  is a positive definite matrix. The optimal solution is  $x^*(\theta) = -P^{-1}\theta$ . We solve this problem using gradient descent with step size  $t$ , whose the fixed-point iterations are

$$z^{k+1} = z^k - t(Pz^k + \theta),$$

which we rewrite in terms of  $z^0$  as

$$z^{k+1} = (I - tP)^{k+1} z^0 - \sum_{i=0}^k (I - tP)^i (t\theta). \tag{9}$$

It is well known that for  $L$ -smooth and  $\mu$ -strongly convex functions, we have

$$\|z^k - z^*\| \leq \tau^k \|z^0 - z^*\|,$$

where  $\tau \in (0, 1)$  as long as  $t \in (0, 2/L)$  and the worst-case convergence rate  $\tau$  is minimized when  $t = 2/(\mu + L)$  [BV04, Chapter 9][Nes18, Chapter 2]. When replacing the distance to optimality  $\|z^0 - z^*\|$  with the fixed-point residual  $\|z^k - z^{k-1}\|$ , the same value of  $t$  minimizes the upper bound, as shown in Proposition 3.1, whose proof is delayed to Appendix A.

**Proposition 3.1.** *Let  $0 < \mu \leq L$ ,  $t > 0$ , and  $\tau = \max\{|1 - t\mu|, |1 - tL|\}$ . For any  $L$ -smooth and  $\mu$ -strongly convex function and gradient descent with fixed step size  $t$ , we have*

$$\|z^k - z^{k-1}\| \leq \tau^{k-1}(1 + \tau) \|z^0 - z^*\|,$$

and the worst-case upper bound is minimized for  $t = 2/(\mu + L)$ .

To form the verification problem and analyze (9), we define

$$H = (I - tP)^K - (I - tP)^{K-1}, \quad E = -t(I - tP)^{K-1}.$$

The verification problem becomes

$$\begin{aligned} & \text{maximize} && \|Hz^0 + E\theta\|^2 \\ & \text{subject to} && z^0 \in Z, \quad \theta \in \Theta. \end{aligned} \tag{10}$$

If  $Z$  and  $\Theta$  are representable with quadratic constraints (e.g., ellipsoidal sets), problem (10) is a nonconvex [quadratically constrained quadratic program \(QCQP\)](#). For this section, let the initial iterate set be the  $\ell_2$ -ball  $Z = \{z \in \mathbf{R}^d \mid \|z - c_z\|_2 \leq r_z\}$  with center  $c_z \in \mathbf{R}^d$  and radius  $r_z \geq 0$ , and the parameter set be the  $\ell_2$ -ball  $\Theta = \{\theta \in \mathbf{R}^p \mid \|\theta - c_\theta\|_2 \leq r_\theta\}$  with center  $c_\theta \in \mathbf{R}^p$  and radius  $r_\theta \geq 0$ . With these sets, we rewrite problem (10) as:

$$\begin{aligned} & \text{maximize} && \|Hz^0 + E\theta\|^2 \\ & \text{subject to} && \|z^0 - c_z\|_2 \leq r_z, \quad \|\theta - c_\theta\|_2 \leq r_\theta. \end{aligned} \tag{11}$$

To derive a convex problem, we lift the problem into a higher dimension and construct a [SDP](#) reformulation [PB17, Section 3.3] [WKK21, Section 2]. When there is only one quadratic constraint, the S-Lemma guarantees tightness of the [SDP](#) relaxations [Yak71, PT07]. We now showcase three examples with only one quadratic constraint so that the S-Lemma holds and we can reformulate the verification problem as a convex [SDP](#). In particular, for each of these experiments we will set either  $r_z = 0$  or  $r_\theta = 0$  to reduce either  $Z$  or  $\Theta$ , respectively, to be a singleton. For consistency, we choose  $t = 2/(\mu + L)$  across all examples and we compare our results with the solutions using the PEP framework.

**Initial iterate set comparison.** First, we isolate the effect of the initial iterate sets only, by setting  $r_\theta = 0$ . In this case, we can rewrite the verification problem (11) as

$$\begin{aligned} & \text{maximize} && \|Hz^0 + Ec_\theta\|^2 \\ & \text{subject to} && \|z^0 - c_z\|_2 \leq r_z. \end{aligned} \tag{12}$$

By squaring the constraints and expanding the objective, we can rewrite problem (12) as

$$\begin{aligned} & \text{maximize} && (z^0)^T H^T H z^0 + 2(Ec_\theta)^T H z^0 + (Ec_\theta)^T Ec_\theta \\ & \text{subject to} && (z^0)^T z^0 - 2c_z^T z^0 \leq r_z^2 - c_z^T c_z. \end{aligned} \tag{13}$$

To get a convex formulation, given a general quadratic form  $v^T J v$  with  $v \in \mathbf{R}^d$ , we can write

$$v^T J v = \mathbf{tr}(v^T J v) = \mathbf{tr}(J v v^T) = \mathbf{tr}(J M),$$

where the second equality follows from the cyclic property of the trace, and in the last equality we introduce a matrix variable  $M = v v^T$ . We relax this rank-one constraint to an inequality constraint  $M \succeq v v^T$  and note that

$$M \succeq v v^T \iff \begin{bmatrix} M & v \\ v^T & 1 \end{bmatrix} \succeq 0, \quad (14)$$

where the equivalence holds due to the Schur complement [BV04, Section B.2]. With this technique, we derive our convex reformulation of problem (12) as the following SDP:

$$\begin{aligned} & \text{maximize} && \mathbf{tr}(H^T H M) + 2(E c_\theta)^T H z^0 + (E c_\theta)^T E c_\theta \\ & \text{subject to} && \mathbf{tr}(M) - 2c_z^T z^0 \leq r_z^2 - c_z^T c_z \\ & && \begin{bmatrix} M & z^0 \\ (z^0)^T & 1 \end{bmatrix} \succeq 0. \end{aligned} \quad (15)$$

To show the effect of the initial iterates set, we set  $\Theta = \{0\}$  and, therefore, the optimal solution  $x^* = 0$ . For simplicity, let  $P = \mathbf{diag}(\mu, L)$  with  $\mu = 1, L = 10$ . We first solve the verification problem SDP (15) with initial set  $\bar{Z} = \{z \in \mathbf{R}^2 \mid \|z\| \leq 1\}$  (i.e.  $c_z = 0, r_z = 1$ ) and let  $\bar{z}$  be the worst-case initial iterate. Then, we solve the verification problem SDP with three smaller initial sets. First, we have  $Z_1 = \{z \in \mathbf{R}^2 \mid \|z - 0.9\bar{z}\| \leq 0.1\}$ , which is explicitly constructed to contain the worst-case iterate for the larger initial set  $\bar{Z}$ . Then, we set  $Z_2 = \{z \in \mathbf{R}^2 \mid \|z - c_2\| \leq 0.1\}$  with  $c_2 = (0.842, -0.317)$ , and  $Z_3 = \{z \in \mathbf{R}^2 \mid \|z - c_3\| \leq 0.1\}$  with  $c_3 = (-0.397, -0.807)$ . Note that  $c_2$  and  $c_3$  are two randomly generated vectors with 2-norm equal to 0.9. Lastly, we also compare with the worst-case iterate from the PEP framework with initial condition  $\|z^0 - z^*\|^2 \leq 1$ . Results are shown in Figure 1.

**Parameter set comparison.** For this example, we isolate the effect of the parameter sets only, by setting  $r_z = 0$ . We follow a similar derivation as in the initial iterate set comparison experiment and arrive at the following verification problem SDP:

$$\begin{aligned} & \text{maximize} && \mathbf{tr}(E^T E M) + 2(H c_z)^T E \theta + (H c_z)^T H c_z \\ & \text{subject to} && \mathbf{tr}(M) - 2c_\theta^T \theta \leq r_\theta^2 - c_\theta^T c_\theta \\ & && \begin{bmatrix} M & \theta \\ \theta^T & 1 \end{bmatrix} \succeq 0. \end{aligned} \quad (16)$$

In this example, we fix the initial set to  $Z = \{z^0\}$  with  $z^0 = (1/2, 1/2)$  and consider two different sets for  $\Theta$ . We again consider the same  $P$  as in the previous example. Let  $\Theta_1 = \{\theta \in \mathbf{R}^2 \mid \|\theta - (1, 0)\|_2 \leq 1/4\}$  and  $\Theta_2 = \{\theta \in \mathbf{R}^2 \mid \|\theta - (0, 1)\|_2 \leq 1/4\}$ . We solve

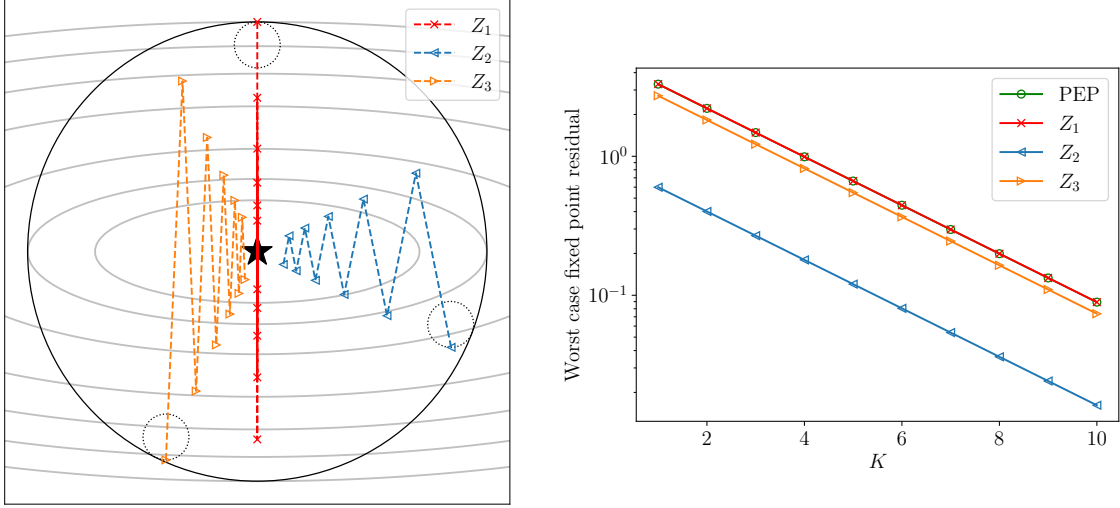


Figure 1: Unconstrained QP experiment with different the initial iterate sets (dashed circles). On the left, we show the iterate paths, and on the right, we plot the worst cast fixed-point residuals for up to  $K = 10$  steps. We also solve the PEP SDP with initial distance to optimality bounded by 1 (solid black circle). The verification problem and PEP agree on the worst-case value for  $Z_1$ .

the verification problem [SDP](#) given by (16) with both  $\Theta_1$  and  $\Theta_2$ , and extract the worst-case parameters,  $\theta_1^*$  and  $\theta_2^*$ , and corresponding worst-case iterates,  $z_1^* = -P^{-1}\theta_1^*$  and  $z_2^* = -P^{-1}\theta_2^*$ . Then, we compare solve the PEP problem with distance from optimality  $R^2 = \max\{\|(1, 0) - z_1^*\|^2, \|(0, 1) - z_2^*\|^2\}$ . Results are shown in Figure 2.

**Quadratic term comparison.** Lastly, we set  $\Theta = \{0\}$  and  $Z = \{z \in \mathbf{R}^2 \mid \|z\| \leq 1\}$ , and vary  $P$  while maintaining the smoothness and strong convexity parameters. To achieve this, we randomly sample orthogonal matrices  $Q_1, Q_2$  and define  $P_1 = Q_1 P Q_1^T$  and  $P_2 = Q_2 P Q_2^T$ . Since we set  $\Theta = \{0\}$ , the verification problem [SDP](#) is again of the form (15), and  $P_1, P_2$  enter into the problem through  $H$  and  $E$ . We solve the verification problem [SDP](#) with  $P_1$  and  $P_2$  and show the results in Figure 3, in comparison with the PEP framework.

## 4 Convex relaxation

### 4.1 NP-hardness

Besides the gradient descent examples for unconstrained QPs presented in Section 3.1, where the  $S$ -lemma provides tight [SDP](#) relaxations, it is in general  $\mathcal{NP}$ -hard to solve problem (VP), as shown in Theorem 4.1, whose proof appears in Appendix B.1.

**Theorem 4.1.** *The performance verification problem (VP) is  $\mathcal{NP}$ -hard.*

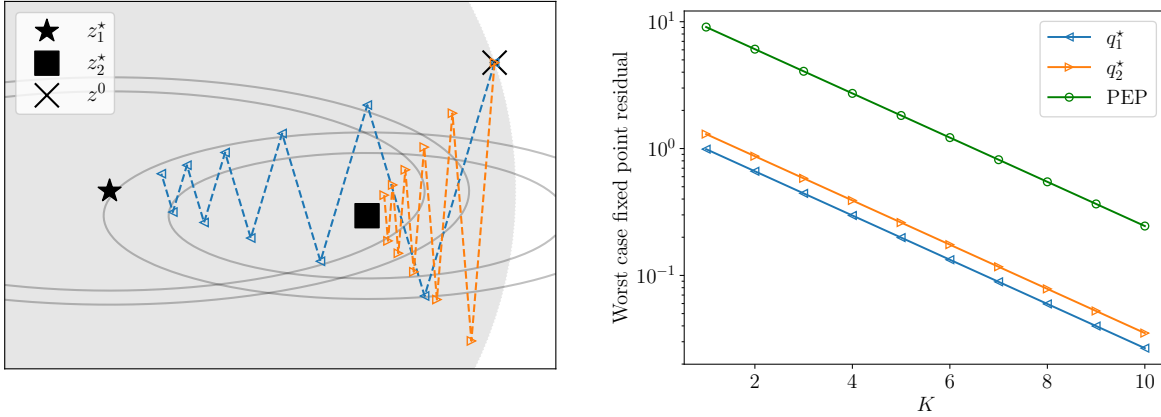


Figure 2: Unconstrained QP example with two parameter sets and fixed initial iterate  $z^0$ . On the left, we show the iterate paths for the worst-case parameter values together with the contour plots of the worst-case functions. The shaded gray area represents the initial condition for the PEP problem, which is large enough to include the initial iterate  $z^0$ . On the right we plot the worst-case fixed-point residuals for  $K = 10$  steps.

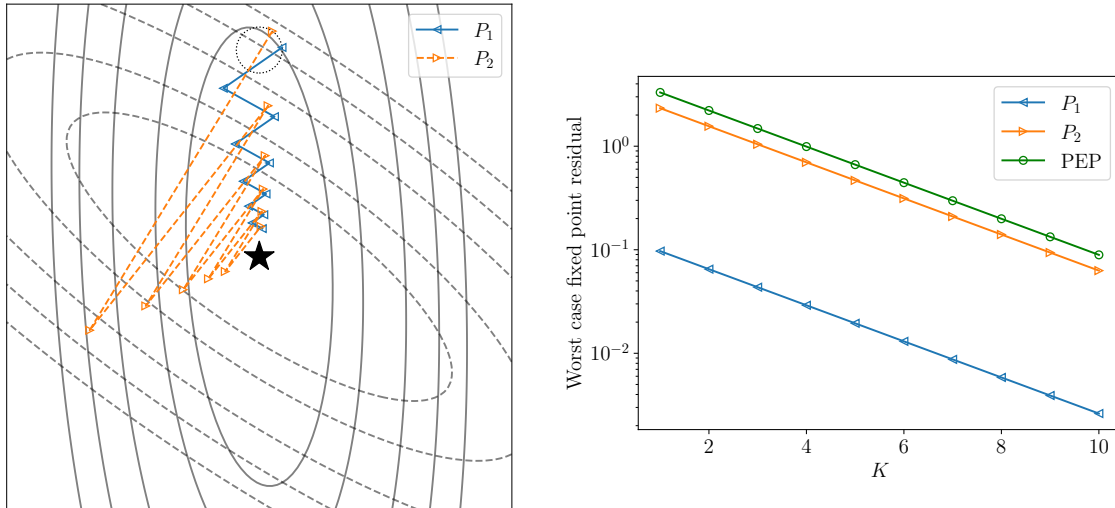


Figure 3: Unconstrained QP example with two different quadratic terms. On the left, we show the worst-case iterate paths for up to  $K = 10$  steps. On the right, we compare the worst-case residuals to those from the PEP SDP.

In the following sections, we derive strong relaxations for the performance verification problem, by replacing nonconvex components in objective and constraints with semidefinite constraints that are linear in the matrix variables. With this procedure, we can compute upper bounds to the optimal value of problem (VP). For each set described in this section, we represent the original constraints as set  $F$  and the lifted constraints as set  $G$ .

## 4.2 Objective

Proposition 4.1 shows how we replace the quadratic objective  $\|z^K - z^{K-1}\|_2^2$  with a linear objective in the new matrix variables together with a positive semidefinite constraint to obtain an upper bound. The proof appears in Appendix B.2.

**Proposition 4.1** (objective reformulation). *Consider functions  $f : \mathbf{R}^d \times \mathbf{R}^d \rightarrow \mathbf{R}$  and  $g : \mathbf{S}^{2d \times 2d} \rightarrow \mathbf{R}$  defined as*

$$f(x, y) = \|x - y\|_2^2,$$

$$g(M) = \text{tr} \left( \begin{bmatrix} I & -I \\ -I & I \end{bmatrix} M \right) \quad \text{with} \quad \begin{bmatrix} M & x \\ x^T & y \\ y^T & 1 \end{bmatrix} \succeq 0.$$

Then,  $g(M) \geq f(x, y)$ .

## 4.3 Primitive algorithm steps

Since all fixed-point iteration steps we consider can be written in terms of affine and element-wise maximum steps (Section 2.1), we describe their reformulation in detail.

**Affine.** For an affine step (5) of the form  $Dy = Ax + Bq(\theta)$ , we can directly enforce the linear equalities as constraints of the verification problem. However, as shown in Proposition 4.1, we introduce new matrix variables in the SDP relaxation. To bound the new matrix variables that correspond to affine steps, we self-multiply the constraints:

$$(Dy)(Dy)^T = (Ax + Bq(\theta))(Ax + Bq(\theta))^T, \quad (17)$$

and this allows us to derive constraints on the matrix variables [PB17, JL20]. Similarly to equation (14), we linearize the vector products by introducing new matrix variables, as shown in Proposition 4.2, which we prove in Appendix B.3.

**Proposition 4.2** (affine step). *Consider matrices  $A \in \mathbf{R}^{d \times d}$ ,  $B \in \mathbf{R}^{d \times n}$ ,  $D \in \mathbf{R}^{d \times d}$ , where*

$D$  is invertible. Let

$$F = \{(y, x, q) \in \mathbf{R}^d \times \mathbf{R}^d \times \mathbf{R}^n \mid Dy = Ax + Bq\}, \quad \text{and}$$

$$G = \left\{ (y, x, q) \in \mathbf{R}^d \times \mathbf{R}^d \times \mathbf{R}^n \left| \begin{array}{l} \exists M_1 \in \mathbf{S}^{d \times d}, M_2 \in \mathbf{S}^{(d+n) \times (d+n)} \text{ such that} \\ Dy = Ax + Bq, \\ DM_1 D^T = \begin{bmatrix} A & B \end{bmatrix} M_2 \begin{bmatrix} A^T \\ B^T \end{bmatrix}, \\ \begin{bmatrix} M_1 & y \\ y^T & 1 \end{bmatrix} \succeq 0, \quad \begin{bmatrix} M_2 & x \\ x^T & q^T & 1 \end{bmatrix} \succeq 0 \end{array} \right. \right\}.$$

Then,  $F \subseteq G$ .

**Element-wise maximum.** For element-wise maximum steps (6) of the form  $y = \max\{x, l\}$ , we can relax the constraints using Proposition 4.3, that we prove in Appendix B.4.

**Proposition 4.3** (element-wise maximum step). *Let*

$$F = \{(y, x, l) \in \mathbf{R}^d \times \mathbf{R}^d \times \mathbf{R}^d \mid y = \max\{x, l\}\}, \quad \text{and}$$

$$G = \left\{ (y, x, l) \in \mathbf{R}^d \times \mathbf{R}^d \times \mathbf{R}^d \left| \begin{array}{l} \exists M \in \mathbf{S}^{3d \times 3d} \text{ such that} \\ y \geq x, y \geq l, \\ \text{tr} \left( \begin{bmatrix} I & -I/2 & -I/2 \\ -I/2 & 0 & I/2 \\ -I/2 & I/2 & 0 \end{bmatrix} M \right) = 0, \\ \begin{bmatrix} M & y \\ M & x \\ M & l \\ y^T & x^T & l^T & 1 \end{bmatrix} \succeq 0. \end{array} \right. \right\}.$$

Then,  $F \subseteq G$ .

All proximal steps considered in this work can be written in terms of these two core steps, as discussed in Section 2.2. We summarize the proximal algorithm steps from Section 2.2 and their corresponding relaxations in Table 1.

#### 4.4 Initial iterate and parameter sets

While the sets in Section 2.3 are convex, we now express them in terms of the lifted SDP variables by introducing additional constraints to obtain tight SDP relaxations for problem (VP).

Table 1: Proximal algorithm steps for solving [parametric quadratic programs](#) [PB13, §6].

$f$	$z = \mathbf{prox}_{\lambda f}(v)$	Constraints	Lifted Constraints
$x^T Ax + b^T x$	$z = (A + \lambda I)^{-1}(v - b)$	$(A + \lambda I)z = v - b$	$(A + \lambda I)z = v - b,$ $(A + \lambda I)M_1(A + \lambda I)^T = \begin{bmatrix} I & -I \\ -I & \end{bmatrix} M_2 \begin{bmatrix} I \\ -I \end{bmatrix},$ $\begin{bmatrix} M_1 & z \\ z^T & 1 \end{bmatrix} \succeq 0, \begin{bmatrix} M_2 & v \\ v^T & b^T & 1 \end{bmatrix} \succeq 0$
$I_{\mathbf{R}_+^n}$	$z = (v)_+$	$z \geq 0, z \geq v,$ $z^T(z - v) = 0$	$z \geq 0, z \geq v,$ $\mathbf{tr} \left( \begin{bmatrix} I & -I/2 \\ -I/2 & 0 \end{bmatrix} M \right) = 0,$ $\begin{bmatrix} M & z \\ z^T & v^T & 1 \end{bmatrix} \succeq 0$
$I_{[l,u]}$	$z = \min \{u, \max \{v, l\}\}$	$y \geq l, y \geq v,$ $(y - l)^T(y - v) = 0$ $z \leq u, z \leq y,$ $(u - z)^T(y - z) = 0$	$y \geq l, y \geq v, z \leq u, z \leq y,$ $\mathbf{tr} \left( \begin{bmatrix} I & -I/2 & -I/2 \\ -I/2 & 0 & I/2 \\ -I/2 & I/2 & 0 \end{bmatrix} M_1 \right) = 0,$ $\mathbf{tr} \left( \begin{bmatrix} I & -I/2 & -I/2 \\ -I/2 & 0 & I/2 \\ -I/2 & I/2 & 0 \end{bmatrix} M_2 \right) = 0,$ $\begin{bmatrix} & y \\ M_1 & v \\ & l \\ y^T & v^T & l^T & 1 \end{bmatrix} \succeq 0, \begin{bmatrix} & z \\ M_2 & y \\ & u \\ z^T & y^T & u^T & 1 \end{bmatrix} \succeq 0$
$\ x\ _1$	$z = \max\{v, \lambda\} - \max\{-v, \lambda\}$	$y \geq \lambda, y \geq v$ $(y - \lambda)^T(y - v) = 0$ $w \geq \lambda, w \geq -v$ $(w - \lambda)^T(w + v) = 0$ $z = y - w$	$y \geq \lambda, y \geq v, w \geq \lambda, w \geq -v, z = y - w,$ $\mathbf{tr} \left( \begin{bmatrix} I & -I/2 & -(1/2)\mathbf{1} \\ -I/2 & 0 & (1/2)\mathbf{1} \\ -(1/2)\mathbf{1}^T & (1/2)\mathbf{1}^T & 0 \end{bmatrix} M_1 \right) = 0,$ $\mathbf{tr} \left( \begin{bmatrix} I & I/2 & -(1/2)\mathbf{1} \\ I/2 & 0 & -(1/2)\mathbf{1} \\ -(1/2)\mathbf{1}^T & -(1/2)\mathbf{1} & 0 \end{bmatrix} M_2 \right) = 0,$ $M_3 = \begin{bmatrix} I & -I \\ -I & \end{bmatrix} M_4 \begin{bmatrix} I \\ -I \end{bmatrix},$ $\begin{bmatrix} & y \\ M_1 & v \\ & \lambda \\ y^T & v^T & \lambda & 1 \end{bmatrix} \succeq 0, \begin{bmatrix} & w \\ M_2 & v \\ & \lambda \\ w^T & v^T & \lambda & 1 \end{bmatrix} \succeq 0$ $\begin{bmatrix} M_3 & z \\ z^T & 1 \end{bmatrix} \succeq 0, \begin{bmatrix} & z \\ M_4 & y \\ & w \\ z^T & y^T & w^T & 1 \end{bmatrix} \succeq 0$

**Hypercubes.** For hypercubes, we derive constraints using Proposition 4.4, whose proof appears in Appendix B.5.

**Proposition 4.4** (hypercubes). *Consider vectors  $l, u \in \mathbf{R}^d$ . Let*

$$F = \{z \in \mathbf{R}^d \mid l \leq z \leq u\}, \quad \text{and}$$

$$G = \left\{ z \in \mathbf{R}^d \mid \exists M \in \mathbf{S}^{d \times d} \text{ such that } uz^T - ul^T - M + zl^T \geq 0, \quad \begin{bmatrix} M & z \\ z^T & 1 \end{bmatrix} \succeq 0 \right\}.$$

Then,  $F \subseteq G$ .

**Polyhedra.** For polyhedral constraints, we derive constraints using Proposition 4.5, which we prove in Appendix B.6.

**Proposition 4.5** (polyhedra). *Consider  $A \in \mathbf{R}^{m \times d}$ ,  $b \in \mathbf{R}^m$ . Let*

$$F = \{z \in \mathbf{R}^d \mid Az \leq b\}, \quad \text{and}$$

$$G = \left\{ z \in \mathbf{R}^d \mid \begin{array}{l} \exists M \in \mathbf{S}^{m+d}, s \in \mathbf{R}^m \text{ such that} \\ Az + s = b, s \geq 0 \\ \begin{bmatrix} A & I \end{bmatrix} M \begin{bmatrix} A^T \\ I \end{bmatrix} = bb^T, \quad \begin{bmatrix} M & z \\ z^T & s^T \\ & & 1 \end{bmatrix} \succeq 0, \end{array} \right\}.$$

Then,  $F \subseteq G$ .

**$\ell_p$ -ball.** We handle the cases where  $p = 1, 2, \infty$  separately as each one requires different types of constraints. For  $p = 1$ , we introduce an auxiliary variable  $u \in \mathbf{R}^d$  to encode  $\|z^0 - c\|_1 \leq r$  with the following linear constraints,

$$z^0 - c \leq u, \quad -z^0 + c \leq u, \quad \mathbf{1}^T u \leq r.$$

By considering the stacked variable  $(z^0, u)$ , we obtain a polyhedral constraint with

$$A = \begin{bmatrix} I & -I \\ -I & -I \\ 0 & \mathbf{1}^T \end{bmatrix}, \quad b = \begin{bmatrix} c \\ -c \\ r \end{bmatrix}.$$

which we can reformulate with Proposition 4.5. The case of  $p = \infty$  corresponds to a hypercube with  $l = c - r\mathbf{1}$  and  $u = c + r\mathbf{1}$ , which we can reformulate with Proposition 4.4. For  $p = 2$ , we apply Proposition 4.6, which is proven in Appendix B.7.

**Proposition 4.6** ( $\ell_2$ -ball). Consider  $c \in \mathbf{R}^d$  and  $r \in \mathbf{R}$ . Let

$$F = \{z \in \mathbf{R}^d \mid \|z - c\| \leq r\}, \quad \text{and}$$

$$G = \left\{ z \in \mathbf{R}^d \left| \begin{array}{l} \exists M \in \mathbf{S}^{2d} \text{ such that} \\ \text{tr} \left( \begin{bmatrix} I & -I \\ -I & I \end{bmatrix} M \right) \leq r^2, \quad \begin{bmatrix} M & z \\ z^T & c^T & 1 \end{bmatrix} \succeq 0 \end{array} \right. \right\}.$$

Then,  $F \subseteq G$ .

## 4.5 Tightening the relaxation

To tighten the relaxation, we introduce additional inequalities using the [reformulation-linearization technique \(RLT\)](#) [SA10, Ans09]. The main idea is to combine known bounds on the any problem variable to form valid inequalities involving the new matrix variables. Consider a variable  $z \in \mathbf{R}^d$  and its upper bound  $\bar{z}$  and lower bound  $\underline{z}$ . Analogously to Proposition 4.4, we can rearrange the bound constraints as follows

$$\underline{z} \leq z \leq \bar{z} \quad \iff \quad \begin{aligned} (\bar{z} - z)(\bar{z} - z)^T &\geq 0 \\ (z - \underline{z})(z - \underline{z})^T &\geq 0 \\ (\bar{z} - z)(z - \underline{z})^T &\geq 0 \end{aligned}$$

where we cross-multiplied the lower and upper bound inequalities. By replacing products  $zz^T$  with the symmetric positive semidefinite matrix  $M \in \mathbf{S}_+^d$ , we obtain constraints

$$\begin{aligned} \bar{z}\bar{z}^T - \bar{z}z^T - z\bar{z}^T + M &\geq 0 \\ M - z\underline{z}^T - \underline{z}z^T + \underline{z}\underline{z}^T &\geq 0 \\ \bar{z}z^T - \bar{z}\underline{z}^T - M + z\underline{z}^T &\geq 0 \\ M &\succeq 0, \end{aligned} \tag{18}$$

which we directly include in our relaxation. Note that the constraint  $\underline{z} \leq z \leq \bar{z}$  is for these constraints [SA10, Proposition 1]. By knowing the upper and lower bounds on the problem variables, this procedure allows us to tighten the relaxation in terms of the lifted variables.

**Bound propagation.** The [RLT](#) requires lower and upper bounds on every variable in order to construct tightening inequalities. First, we use the initial sets  $Z, \Theta$  to derive bounds on the initial iterate  $z^0$  and parameter  $\theta$ . When the sets are either hypercubes or  $\ell_p$ -ball sets, the initial bounds can be efficiently computed. In the hypercube case,  $Z = \{z \mid l \leq z \leq u\}$ , the initial bounds are given by  $\underline{z} = l$ ,  $\bar{z} = u$ . In the  $\ell_p$ -ball case,  $Z = \{z \mid \|z - c\|_p \leq r\}$ , the initial bounds are given by  $\underline{z} = c - r$ ,  $\bar{z} = c + r$ .

We need to efficiently propagate these initial bounds across the iterate steps.

- **Affine steps.** First consider an affine step  $Dy = Ax + Bq(\theta)$  with known lower bounds  $\underline{x}, \underline{q}(\theta)$  and upper bounds  $\bar{x}, \bar{q}(\theta)$ . To propagate these bounds on  $y$ , we use the invertibility assumption of  $D$  and write

$$y = \tilde{A}x + \tilde{B}q(\theta), \quad (19)$$

where we compute  $\tilde{A} = D^{-1}A$  and  $\tilde{B} = D^{-1}B$  using a factorization of matrix  $D$ . We now bound the terms in equation (19) individually and then sum the bounds together as commonly done in *interval arithmetic* [GDS<sup>+</sup>18]. Given bounds on  $x$  denoted by  $\underline{x}, \bar{x}$ , the bounds for  $\tilde{A}x$  are computed via [GDS<sup>+</sup>18, Section 3]:

$$\begin{aligned} \tilde{A}x &\leq (1/2) \left( \tilde{A}(\bar{x} + \underline{x}) + |\tilde{A}|(\bar{x} - \underline{x}) \right) \\ \tilde{A}x &\geq (1/2) \left( \tilde{A}(\bar{x} + \underline{x}) - |\tilde{A}|(\bar{x} - \underline{x}) \right), \end{aligned} \quad (20)$$

where  $|\tilde{A}|$  is the element-wise absolute value of  $\tilde{A}$ .

If  $x$  lives in an  $\ell_p$ -ball of radius  $r$  centered at  $c$ , then we can construct tighter bounds on each component of  $\tilde{A}x$  as follows [XSZ<sup>+</sup>20, Section 3.2]:

$$\begin{aligned} (\tilde{A}x)_i &\leq r \left\| \tilde{A}_i^T \right\|_q + \tilde{A}_i^T c \\ (\tilde{A}x)_i &\geq -r \left\| \tilde{A}_i^T \right\|_q + \tilde{A}_i^T c, \end{aligned} \quad (21)$$

for  $i = 1, \dots, d$ . Here, where  $\tilde{A}_i^T$  is the  $i$ -th row of  $\tilde{A}$  and  $q$  is the dual norm of  $p$  satisfying  $1/p + 1/q = 1$ . We can use (20) or (21) to bound  $\tilde{B}q(\theta)$  in a similar way.

- **Element-wise maximum steps.** Consider an element-wise maximum step given by  $y = \max\{x, l(\theta)\}$ . With known lower bounds  $\underline{x}, \underline{l}(\theta)$  and upper bounds  $\bar{x}, \bar{l}(\theta)$ , we can compute bounds on  $y$ . Since the max function is element-wise nondecreasing, the bounds propagate as [GDS<sup>+</sup>18, Section 3]:

$$\underline{y} = \max\{\underline{x}, \underline{l}(\theta)\}, \quad \bar{y} = \max\{\bar{x}, \bar{l}(\theta)\}. \quad (22)$$

In the verification problem, we use the techniques described by (20), (21), and (22) to derive lower and upper bounds on every variable across all iterations  $k$ . We use these bounds to form **RLT** inequalities and tighten the relaxation.

**Triangle relaxation.** In addition to the variable bounds with **RLT**, we also compute further bounds for the element-wise maximum steps. Consider an element-wise maximum step  $y = \max\{x, l(\theta)\}$ ,  $y, x, l(\theta) \in \mathbf{R}^d$ , with precomputed lower bounds  $\underline{y}, \underline{x}$  and upper bounds  $\bar{y}, \bar{x}$ . Note that the bounds on  $l(\theta)$  enter through the precomputed bounds on  $y$  as shown in (22). We can introduce another valid inequality with the so-called *triangle* relaxation [Ehl17]:

$$y \leq \frac{\bar{y} - \underline{y}}{\bar{x} - \underline{x}}(x - \underline{x}) + \underline{y}, \quad (23)$$

For simplicity, we rewrite (23) as

$$y \leq Ex + c, \quad (24)$$

for diagonal matrix  $E$  and vector  $c$  defined as

$$E_{ii} = \frac{\bar{y}_i - \underline{y}_i}{\bar{x}_i - \underline{x}_i}, \quad c_i = -\frac{\bar{y}_i - \underline{y}_i}{\bar{x}_i - \underline{x}_i} \underline{x}_i + \underline{y}_i,$$

for  $i = 1, \dots, d$ . To incorporate the triangle relaxation into our relaxed problem, we use a similar technique to the [RLT](#) inequalities. That is, we multiply each inequality in (24) by  $\bar{x} - x \geq 0$  to obtain bounds on the matrix variables. Explicitly,

$$(Ex + c - y)(\bar{x} - x)^T \geq 0 \implies Ex\bar{x}^T - Exx^T + c\bar{x}^T - cx^T - y\bar{x}^T + yx^T \geq 0. \quad (25)$$

In Proposition 4.3, we introduce a lifted matrix variable  $M$  for the element-wise maximum steps. We can rewrite the inequalities from (25) in terms of this same  $M$ . The nonnegative expression in (25) is a  $d \times d$  matrix, so we show the constraint corresponding to the  $ij$ -th element. In terms of  $M$  from Proposition 4.3, the inequalities can be written as

$$(\bar{x}_j E_i)^T x + c_i \bar{x}_j - c_i x_j - \bar{x}_j y_i + \mathbf{tr} \left( \begin{bmatrix} 0 & e_i e_j^T & 0 \\ 0 & -E_{ii} e_i e_j^T & 0 \\ 0 & 0 & 0 \end{bmatrix} M \right) \geq 0, \quad i, j = 1, \dots, d, \quad (26)$$

where  $e_i \in \mathbf{R}^d$  equals 1 at index  $i$  and 0 elsewhere. The inequalities in (26) also show that we can reuse the lifted matrix variables. We discuss this idea further in Appendix C.

## 5 Numerical examples

For every experiment, we compare three main metrics:

- **Verification problem SDP objective (VPSDP)**. We solve the SDP relaxation of the verification problem, denoted VPSDP, to compute the upper bound VPSDP on the worst-case fixed-point residual over the variations of initial iterates and problem parameters. We apply the [RLT](#), triangle relaxation, and coupling techniques discussed in Section 4.5 and Appendix C.
- **PEP objective (PEP)**. We compute the worst-case objective from the PEP framework, denoted as PEP. To apply the PEP framework, we need to provide an upper bound  $R$  on the initial distance to optimality, *i.e.*,  $\|z^0 - z^*\|^2 \leq R$ . However, as discussed in Section 3, for every  $\theta$  we have a different  $z^*(\theta)$  and it is not obvious which upper bound to provide. To estimate  $R$ , we consider  $N = 10,000$  problem instances and initial iterates by sampling  $\{(z_i^0, \theta_i)\}_{i=1}^N$  uniformly from the set  $Z \times \Theta$ . For each instance, we solve the [PQP](#) to optimality to find  $z^*(\theta_i)$  and compute  $R = \max_{i=1, \dots, N} \|z_i^0 - z^*(\theta_i)\|$ .

- **Sample maximum objective.** (SM) For each of the  $N$  sampled problems, we also run the first-order method and compute the fixed-point residual for  $k = 1, \dots, K$  steps. We then compute the sample maximum fixed-point residual for each  $k$  and report this as the sample maximum worst-case objective SM. This value serves as a lower bound to both the VPSDP and PEP objectives.

We also report:

- **Computation times for solving VPSDP.** We report the solve time in seconds for each VPSDP.
- **Improvement over PEP.** We measure the improvement of over PEP, we report the ratio between its objective PEP and the objective of our relaxation VPSDP and the lower bound obtained from the sample maximum SM:

$$\frac{\text{PEP}}{\text{VPSDP}} \quad \text{and} \quad \frac{\text{PEP}}{\text{SM}}. \quad (27)$$

We present full numerical results for every experiment in Appendix D.

**Computational scalability.** We use one of our experiments to show the difficulty in solving the nonconvex verification problem exactly. In Section 5.3, we set up and solve the nonconvex verification problem as a QCQPs with a fixed time limit. In doing so, we apply bound propagation techniques to construct lower and upper bounds on each variable. After the time limit, we report the best lower and upper bound on the optimal objective.

**Software.** All examples are written in Python 3.10. To solve the SDPs, we use MOSEK version 10.1, specifically through the MOSEK Fusion API for Python [ApS24]. We set the primal feasibility, dual feasibility, and duality gap tolerances all as  $10^{-7}$ . To compare our verification problem with PEP, we use the PEPit toolbox [GMG<sup>+</sup>22], which interfaces with MOSEK through CVXPY [DB16, AVDB18]. To solve the nonconvex verification problem exactly in Section 5.3, we use Gurobi version 10.0 [Gur22]. All computations were run on the Princeton HPC Della Cluster with 16 CPU cores. The code for all experiments can be found at

[https://github.com/stellatogrp/algorithm\\_verification](https://github.com/stellatogrp/algorithm_verification).

## 5.1 Nonnegative least squares

For a matrix  $A \in \mathbf{R}^{m \times n}$  with  $m \geq n$  and a parameterized vector  $b(\theta) \in \mathbf{R}^m$ , the **nonnegative least squares (NNLS)** problem is defined as:

$$\begin{aligned} & \text{minimize} && (1/2)\|Ax - b(\theta)\|^2 \\ & \text{subject to} && x \geq 0. \end{aligned} \quad (28)$$

---

**Algorithm 1** Projected gradient descent for the [NNLS](#) problem (28).

---

- 1: **Given** step size  $t > 0$ , problem data  $(A, b(\theta))$ ,  $K$  number of iterations, initial iterate  $z^0$
  - 2: **for**  $k = 0, \dots, K - 1$  **do**
  - 3:      $y^{k+1} = (I - tA^T A)z^k + tA^T b(\theta)$
  - 4:      $z^{k+1} = (y^{k+1})_+$
  - 5: **return**  $z^K$
- 

We analyze projected gradient descent with step size  $t > 0$ , presented in Algorithm 1. To choose the step size, we consider the minimum and maximum eigenvalues of  $A^T A$ , denoted  $\mu$  and  $L$ , respectively. It is well-known that, for  $t < 2/L$ , the algorithm converges as the gradient step is a contractive operator [BV04, Chapter 9][Nes18, Chapter 2] and the projection is nonexpansive [RB16, Section 5.1] [PB13, Section 2.3]. Furthermore, when  $\mu > 0$ , choosing  $t^* = 2/(\mu + L)$  is optimal in terms of minimizing the worst-case convergence rate (Proposition 3.1).

We consider two instances where the objective is nonstrongly convex and strongly convex. First, we consider fixed step sizes across  $K$  iterations. Specifically, we grid 5 different step sizes in the range  $[1/L, 2/L]$ , and for the strongly convex case, we additionally include  $t^* = 2/(\mu + L)$ . Second, we consider the silver step size schedule, a method that aims to accelerate gradient descent via carefully selected, non-constant, step sizes [AP23a, AP23b]. The silver step size schedule for strongly convex problems appears in [AP23a, Section 3], and for nonstrongly convex problems appears in [AP23b, Section 2].

**Problem setup.** We randomly generate  $A \in \mathbf{R}^{60 \times 40}$  such that  $\mu = 0$ ,  $L = 100$  for the nonstrongly convex case and  $\mu = 20$ ,  $L = 100$  for the strongly convex case. We choose  $b(\theta)$  to be an  $\ell_2$ -ball of radius 0.5 centered at  $c$ , where  $c_i = 30$ ,  $i = 1, \dots, 30$  and 0 otherwise. For each candidate step size schedule, we run the verification problem with initial iterate set  $Z = \{0\}$ . We run the fixed step size experiments up to  $K = 10$ , and we run the silver step size experiments up to  $K = 7$  as the recursive definition reaches the best performance when  $K$  is one less than a power of two.

**Fixed step size schedule results.** The nonstrongly convex results are presented in Figure 6 and Tables 2 and 3, while the strongly convex results are presented in Figure 4 and Tables 5 and 6. Across the step sizes, our VPSDP shows a significant improvement in the estimate of the worst-case objective over PEP. In particular, in both cases, with a step size  $t = 2/L$ , the PEP bound remains constant for all  $K$ . This implies that there exists an  $L$ -smooth,  $\mu$ -strongly convex function where proximal gradient descent does not converge, which agrees with the classical analysis [BV04, Chapter 9], [Nes18, Chapter 2]. However, our VPSDP captures that proximal gradient descent still converges for these particular PQPs.

In Figure 5, we look at the strongly convex instance at  $K = 4$  across the different step sizes. There is a discrepancy between the step size that gives the lowest PEP bound and the lowest VPSDP bound. When paired with the lower bound from the sample maximum, SM,

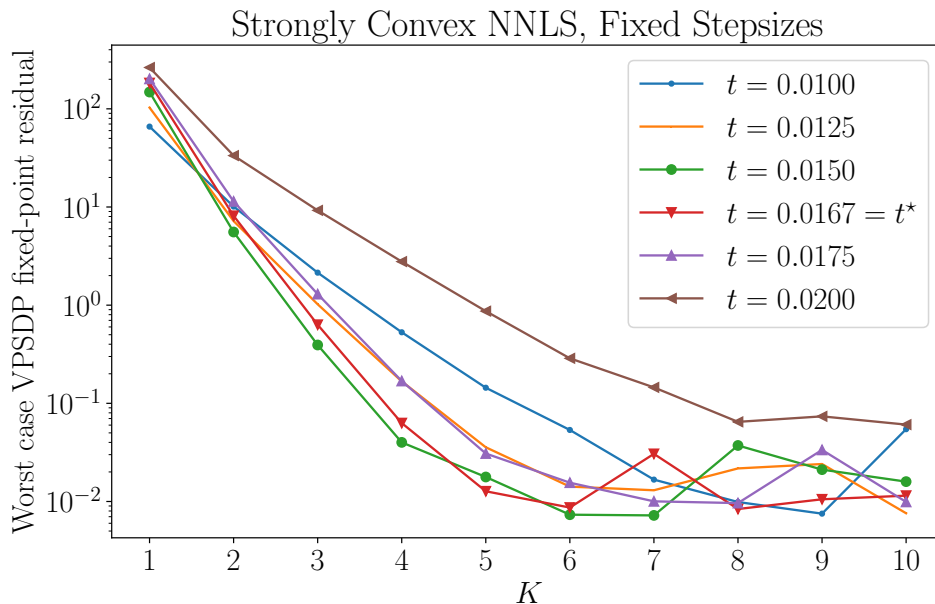


Figure 4: Results for the strongly convex NNLS instance with  $\mu = 20, L = 100$ , for fixed step sizes. Full results are in Tables 5 and 6.

the VPSDP is able to determine the correct step size choice when compared to PEP. The relative scales of the two instances show faster convergence in the strongly convex instance, as expected. When comparing to the sample maximum bound across the step sizes, the VPSDP relaxation gets looser as  $K$  grows. In particular, as the sample maximum fixed point residual gets close to 0, the corresponding VPSDP bound becomes looser.

**Silver step size schedule results.** We present the results with the silver step size schedule for a strongly convex problem in Figure 7 and Table 7, and for a nonstrongly convex problem in Figure 8 and Table 4. In both cases the VPSDP gives a tighter bound compared with PEP. We again observe that the VPSDP relaxation gap gets looser as the sample maximum lower bound approaches 0 for higher values of  $K$ .

Note that the silver schedule derivation was exclusively for smooth unconstrained problems and, as far as we know, its convergence proof has yet to be extended to constrained problems [AP23a, Section 6]. The difficulty arises from the fact that the silver schedule cannot be studied on a per-iteration basis; rather, the entire sequence of gradient steps must be studied together with the interleaved proximal steps. However, our VPSDP analysis offers evidence that the silver schedule can also perform well in constrained settings.

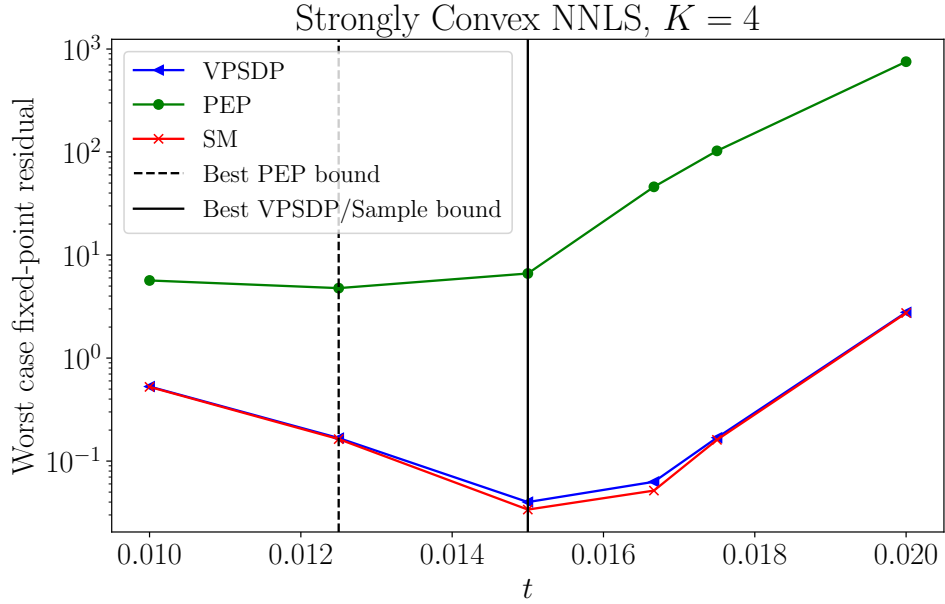


Figure 5: Results to show the effect of  $t$  at  $K = 4$  for the same strongly convex instance as in Figure 4. There is a discrepancy between the PEP and VPSDP bounds on the  $t$  that leads to the smallest residual.

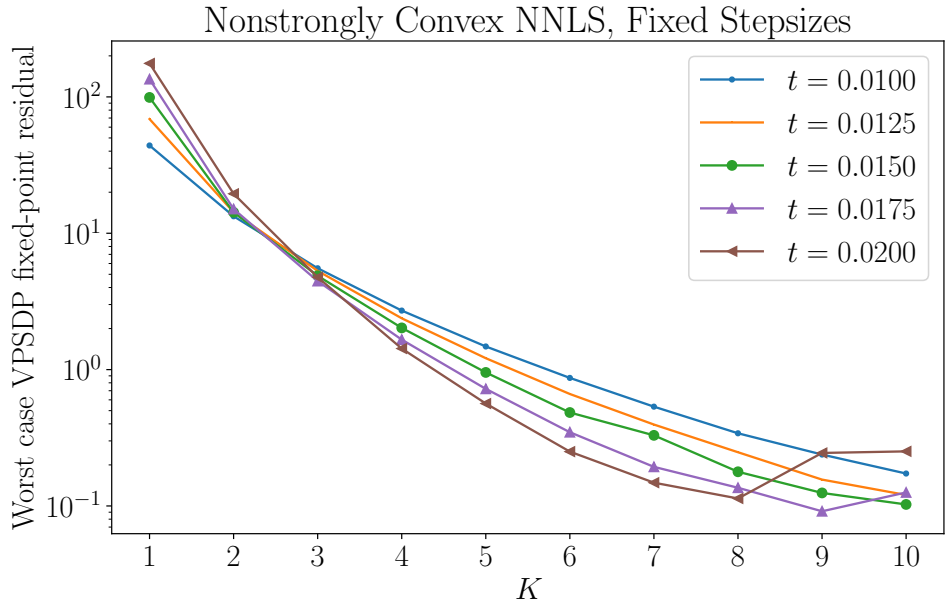


Figure 6: Results for the nonstrongly convex NNLS instance  $L = 100$  for fixed step sizes. Full results are in Tables 2 and 3.

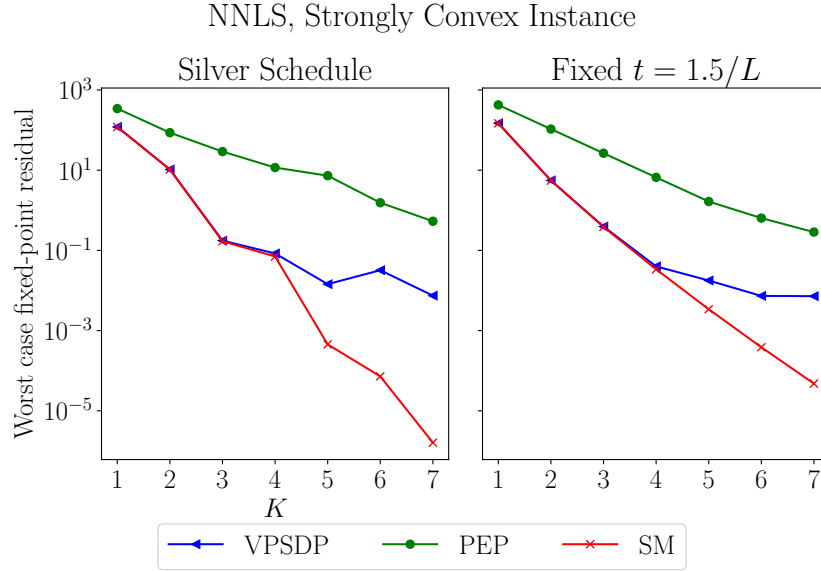


Figure 7: Results for the silver schedule on the strongly convex NNLS instance compared to a single fixed step size schedule. Silver results are presented in Table 7. The VPSDP bound for the silver schedule is lower at  $K = 7$  but the relaxation gets looser as the sample maximum approaches 0.

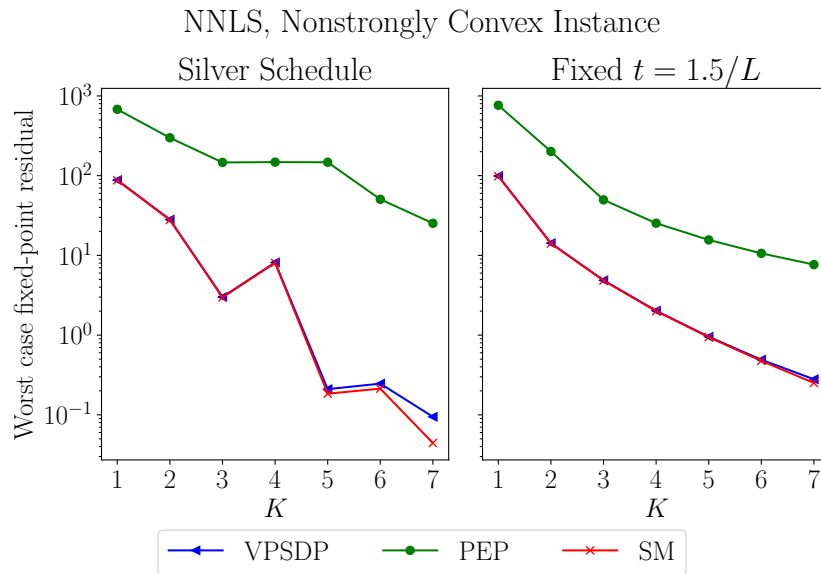


Figure 8: Results for the silver schedule on the nonstrongly convex NNLS instance compared to a single fixed step size schedule. Silver results are presented in Table 4. The VPSDP bound for the silver schedule at  $K = 7$  is lower than the sample maximum bound for the fixed step size case. The overall convergence is slower when compared to the strongly convex case so the relaxation gap is much smaller.

## 5.2 Network utility maximization

Consider a network of  $p$  edges and  $n$  flows, where each edge  $i$  has capacity  $d_i$  for  $i = 1, \dots, p$ , and each flow  $j$  has a nonnegative flow rate  $x_j$  and a maximum value  $s_j$  for  $j = 1, \dots, n$ . Each flow routes over a specific set of edges modeled using a routing matrix  $R \in \{0, 1\}^{p \times n}$ , where  $R_{ij}$  is 1 if flow  $j$  routes through edge  $i$ , and 0 otherwise. The total traffic over each edge is the sum of the flow rates over all flows that pass through it. Therefore, the vector of traffic for every edge is given by  $Rx$ , which is upper-bounded by parametric capacities  $\theta$ , *i.e.*,  $Rx \leq \theta$ . We define the total utility as the sum of linear utilities for each flow, *i.e.*,  $w^T x$  where  $w \in \mathbf{R}^n$  is a fixed vector of weights. Our goal is to choose the flow vector  $x$  that maximizes the total utility across the network, subject to capacity constraints and bounds on the flow. This problem, often referred to as [network utility maximization \(NUM\)](#) [MB10a, Section 1.3.7], can be written as the following parametric LP,

$$\begin{aligned} & \text{minimize} && c^T x \\ & \text{subject to} && Ax \leq b(\theta), \end{aligned} \tag{29}$$

where  $c = -w$ ,  $A^T = [R^T \ -I \ I] \in \mathbf{R}^{m \times n}$  with  $m = p + 2n$ , and  $b(\theta) = (\theta, 0, s) \in \mathbf{R}^{p+2n}$ . By defining the primal-dual iterate  $z = (x, y) \in \mathbf{R}^{n+m}$ , we can write (29) as the following complementarity problem

$$\mathcal{C} \ni z \perp Mz + q \in \mathcal{C}^*, \quad \text{where} \quad M = \begin{bmatrix} 0 & A^T \\ -A & 0 \end{bmatrix} \in \mathbf{R}^{(m+n) \times (m+n)}, \quad q(\theta) = \begin{bmatrix} c \\ b(\theta) \end{bmatrix} \in \mathbf{R}^{m+n},$$

and  $\mathcal{C} = \mathbf{R}^n \times \mathbf{R}_+^m$ . Cone  $\mathcal{C}^* = \{0\}^n \times \mathbf{R}_+^m$  is the dual cone to  $\mathcal{C}$ , defined as  $\mathcal{C}^* = \{w \mid w^T u \geq 0, u \in \mathcal{C}\}$ . We solve this problem using [Douglas-Rachford \(DR\) splitting](#) [DR56, O'D21][SHAS22, Section 3] in the form outlined in Algorithm 2. We use  $\Pi_{\mathcal{C}}(v)$  to denote the projection of a vector  $v \in \mathbf{R}^{n+m}$  onto cone  $\mathcal{C}$  (clipping the negative values in the last  $m$  elements of  $v$  to 0).

---

**Algorithm 2** DR splitting for a general LP problem (29).

---

- 1: **Given** problem data  $(M, q(\theta))$ ,  $K$  number of iterations, initial iterate  $z^0$
  - 2: **for**  $k = 0, \dots, K - 1$  **do**
  - 3:     Solve  $(M + I)u^{k+1} = z^k - q(\theta)$
  - 4:      $\tilde{u}^{k+1} = \Pi_{\mathcal{C}}(2u^{k+1} - z^k)$
  - 5:      $z^{k+1} = z^k + \tilde{u}^{k+1} - u^{k+1}$
  - 6: **return**  $z^K$
- 

In this experiment, we show how our framework can analyze warm-starting strategies by modifying the initial set  $Z$ . In particular, we analyze an application-specific warm-start heuristic to set the initial iterates as follows: every initial flow rate set to the same value being the minimum, across edges, of the ratio between the edge capacity and the number of flows passing through it [MB10a, Section 1.3.7].

**Problem setup.** We create the routing matrix  $R$  with dimensions  $p = 10, n = 5$ , which gives a fixed-point iterate of dimension  $p + 3n = 25$ . For each entry  $R_{ij}$ , we randomly sample a Bernoulli random variable with success probability 0.5. We randomly sample the weight vector  $w$  from a uniform distribution on  $[0, 1]^n$ , the saturation values  $s$  from a uniform distribution on  $[4, 5]^n$ , and the edge capacities  $\theta$  from a uniform distribution over  $\Theta = \{\theta \in \mathbf{R}^n \mid \|\theta - (10)\mathbf{1}\|_2 \leq 0.4\}$ . To obtain a representative primal-dual solution  $\bar{z}$ , we sample one point  $\bar{\theta}$  from  $\Theta$  and solve the resulting LP. We also use  $\bar{\theta}$  to compute the heuristic-based initial iterate  $\tilde{z} = (\alpha\mathbf{1}, 0) \in \mathbf{R}^{n+m}$  where  $\alpha = \min_i \theta_i/k_i$  and  $k_i$  is the number of flows that pass over edge  $i$  [MB10a, Section 1.3.7]. We create three versions of the verification problem and compare the difference between  $Z = \{0\}$  (cold start),  $Z = \{\tilde{z}\}$  (heuristic start), and  $Z = \{\bar{z}\}$  (warm start from representative primal-dual solution). The PEP formulation is the same across these examples, because the problem class and algorithm do not change (see Section 3), with the exception of the radius bounding the initial distance to optimality.

**Results.** We show the results in Figure 9 and Table 8. As implied by the sample maximum bound, the cold start has a lower residual than the heuristic start at  $K = 5$  for this problem setup. Being a heuristic, there is no guarantee that the heuristic start will perform better for every NUM instance. Our verification problem is able to pick up on this fact because of the explicit incorporation of warm-starting.

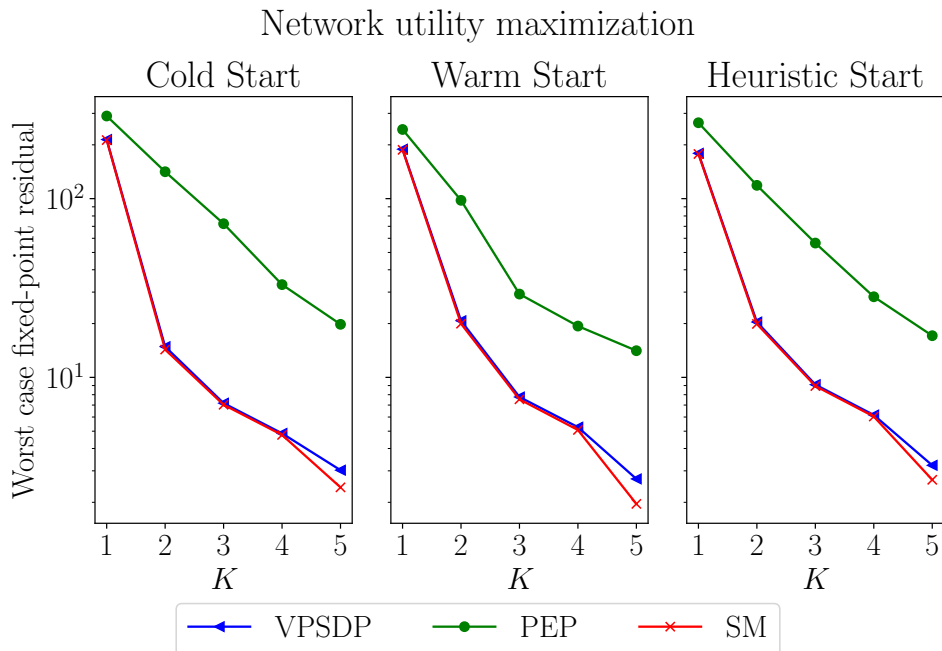


Figure 9: Results for the NUM experiment. For both PEP and VPSDP, the warm start has the tightest bound on the residual. The SM bound shows that VPSDP finds a tighter bound compared to PEP. Full results are in Table 8.

### 5.3 Lasso

To analyze the effect of Nesterov acceleration, we study the  $\ell_1$ -regularized least squares (Lasso) [Tib96] problem,

$$\text{minimize } (1/2)\|Ax - b(\theta)\|^2 + \lambda\|x\|_1, \quad (30)$$

with  $A \in \mathbf{R}^{m \times n}$  and  $b(\theta) \in \mathbf{R}^m$ . We compare the [iterative soft-thresholding algorithm \(ISTA\)](#) and [fast iterative soft-thresholding algorithm \(FISTA\)](#) [BT09, Section 4]. The ISTA is proximal gradient descent using the soft-thresholding function, and is detailed in Algorithm 3. On the other hand, the FISTA is a version of ISTA with carefully chosen momentum updates, and is detailed in Algorithm 4.

---

**Algorithm 3** ISTA for the Lasso problem (30).

---

- 1: **Given** step size  $t > 0$ , problem data  $(A, b(\theta), \lambda)$ ,  $K$  number of iterations, initial iterate  $z^0$ .
  - 2: **for**  $k = 0, \dots, K - 1$  **do**
  - 3:    $y^{k+1} = (I - tA^T A)z^k + tA^T b(\theta)$
  - 4:    $z^{k+1} = \max\{y^{k+1}, \lambda t\} - \max\{-y^{k+1}, \lambda t\}$
  - 5: **return**  $z^K$
- 

---

**Algorithm 4** FISTA for the Lasso problem (30).

---

- 1: **Given** step size  $t > 0$ , problem data  $(A, b(\theta), \lambda)$ ,  $K$  number of iterations, initial iterates  $z^0, w^0$ , and parameter  $\beta_0 = 1$ .
  - 2: **for**  $k = 0, \dots, K - 1$  **do**
  - 3:    $y^{k+1} = (I - tA^T A)w^k + tA^T b(\theta)$
  - 4:    $z^{k+1} = \max\{y^{k+1}, \lambda t\} - \max\{-y^{k+1}, \lambda t\}$
  - 5:    $\beta_{k+1} = (1 + \sqrt{1 + 4\beta_k^2})/2$
  - 6:    $w^{k+1} = z^{k+1} + \beta_k - 1/\beta_{k+1}(z^{k+1} - z^k)$
  - 7: **return**  $z^K$
- 

**Problem setup.** We sample  $A \in \mathbf{R}^{10 \times 15}$  uniformly at random from a standard Normal distribution. We choose  $\lambda = 10$  and parameterize  $b(\theta)$  as an  $\ell_2$ -ball of radius 0.25 centered at  $(10)\mathbf{1}$ . For the step size, we use  $t = 0.04$  for both algorithms. For the initial set, let  $\bar{z}$  be the minimizer of  $(1/2)\|Az - \bar{b}\|_2^2$ , where  $\bar{b}$  is randomly sampled from the parameter set. That is, the least squares solution to a random, unregularized minimization problem. For ISTA, we use  $\{\bar{z}\}$  as the initial set for  $z^0$  and for FISTA, we use  $\{(\bar{z}, \bar{z})\}$  as the initial set for  $(z^0, w^0)$ .

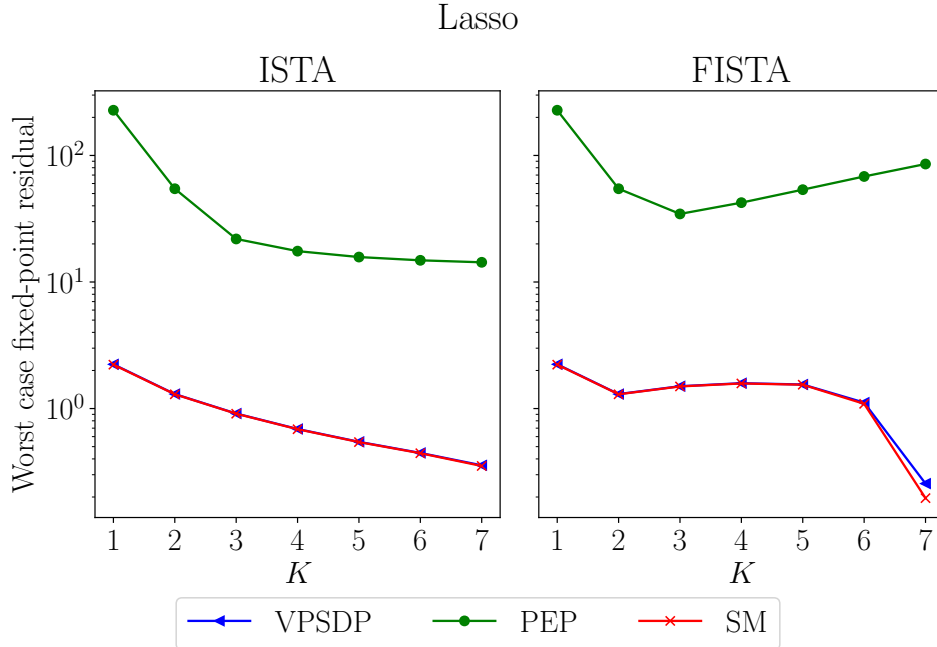


Figure 10: We show the experimental results for a Lasso problem with ISTA vs. FISTA. This shows a parametric family where FISTA outperforms ISTA with  $K = 7$  steps.

**Results.** The results are presented in Figure 10 and Table 9. While FISTA has a larger worst-case fixed-point residual for the middle  $K$  values, it outperforms ISTA at the largest value  $K = 7$ . In this experiment, the VPSDP provide particularly tight bounds, as shown by the sample maximum bound SM. It is also worth noting that the FISTA appears to diverge with PEP, which is consistent with prior results about the convergence of the accelerated proximal gradient descent for nonsmooth objective functions [THG17a, Section 4.2.2].

**Global solver comparison.** Figure 11 and Table 10 show the comparison between VPSDP and Gurobi nonconvex QCQP solver. Since all VPSDPs for Lasso were solved in under an hour, we solved the corresponding exact verification problems in Gurobi with 1% optimality gap a 1 hour time limit. Gurobi is able to find a good incumbent solution, compared to the lower bound SM. We hypothesize that this is because the solver is able to exploit our precomputed lower and upper bounds in the branch and bound search. However, we also observe that the 1 hour time limit is insufficient for the solver to solve the problem to within 1% gap for any  $K \geq 2$ . In addition, the reported gap significantly grows for larger  $K$  values. This shows that, while Gurobi is able to find a good incumbent solution, it struggles to certify optimality.

## Lasso Exact VP Results

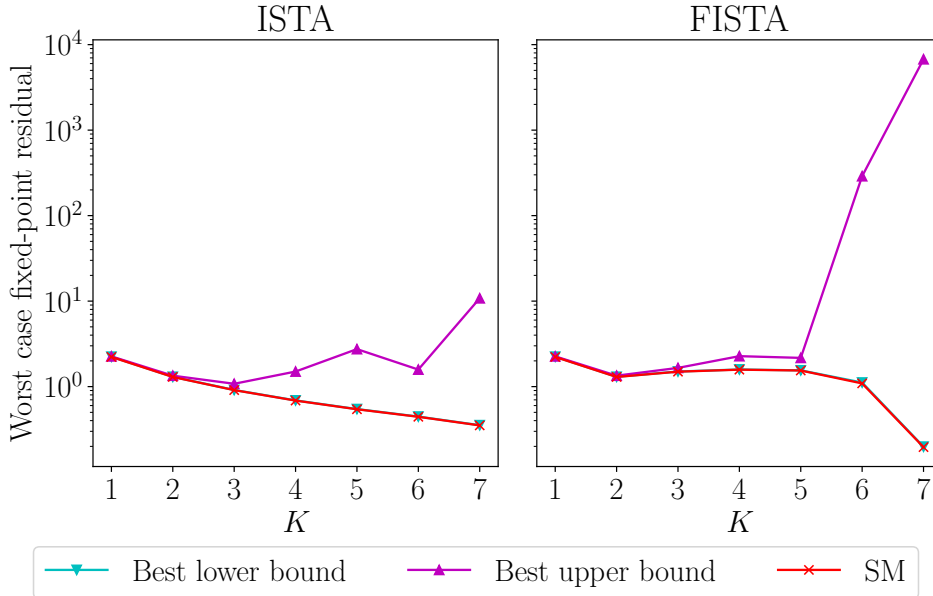


Figure 11: Lasso exact verification problem results after 1 hour solve time. Gurobi as a nonconvex [QCQP](#) solver is able to find the incumbent solution but struggles to verify optimality and tighten the upper bounds for larger values of  $K$ .

### 5.4 Optimal control

Consider the problem of controlling an input-constrained linear dynamical system over a finite time horizon [[BBM17](#), Chapter 8.1]. The system is a vehicle, modeled as a point mass in the 2D plane, to approach the origin. We discretize the dynamics with sampling time  $h$ , obtaining a finite horizon discretization indexed as  $t = 1, \dots, T$ . We define the system state as  $s_t = (p_t, v_t) \in \mathbf{R}^4$ , where  $p_t \in \mathbf{R}^2$  represents the position, and  $v_t \in \mathbf{R}^2$  the velocity at time  $t$ . We observe the output  $y_t = p_t$ . The input  $u_t \in \mathbf{R}^2$  is the force applied to the system with mass  $m$  and friction coefficient  $\eta$ . We can write the linear dynamics as [[BV18](#), Chapter 17.2]

$$s_{t+1} = A^{\text{dyn}} s_t + B^{\text{dyn}} u_t, \quad y_t = C s_t,$$

for  $t = 1, \dots, T$ , with

$$A^{\text{dyn}} = \begin{bmatrix} 1 & 0 & h & 0 \\ 0 & 1 & 0 & h \\ 0 & 0 & 1 - h\eta/m & 0 \\ 0 & 0 & 0 & 1 - h\eta/m \end{bmatrix}, \quad B^{\text{dyn}} = \begin{bmatrix} 0 & 0 \\ 0 & 0 \\ h/m & 0 \\ 0 & h/m \end{bmatrix}, \quad \text{and} \quad C = \begin{bmatrix} 1 & 0 & 0 & 0 \\ 0 & 1 & 0 & 0 \end{bmatrix}.$$

Our goal is to minimize the sum of the output deviations with respect to a reference position  $y^{\text{ref}} \in \mathbf{R}^2$  and input efforts over the time horizon, *i.e.*,  $\sum_{t=1}^T \|y_t - y^{\text{ref}}\|^2 + \gamma \sum_{t=1}^{T-1} \|u_t\|^2$ .

We bound the maximum value of the inputs with  $u^{\max}$ , *i.e.*,  $\|u_t\|_{\infty} \leq u^{\max}$ , and the maximum consecutive input variations (slew rate) by  $d^{\max}$ , *i.e.*,  $\|u_t - u_{t-1}\| \leq d^{\max}$ . The optimal control problem can be written as

$$\begin{aligned}
& \text{minimize} && \sum_{t=1}^T \|Cs_t - y^{\text{ref}}\|^2 + \gamma \sum_{t=1}^{T-1} \|u_t\|^2 \\
& \text{subject to} && s_{t+1} = A^{\text{dyn}}s_t + B^{\text{dyn}}u_t, \quad t = 1, \dots, T-1 \\
& && \|u_t\|_{\infty} \leq u^{\max}, \quad \|u_t - u_{t-1}\|_{\infty} \leq d^{\max}, \quad t = 1, \dots, T-1 \\
& && s_1 = \bar{s}.
\end{aligned} \tag{31}$$

where  $\bar{s}$  is the initial state and  $u_0$  the previous control input. Together, they represent the problem parameters  $\theta = (\bar{x}, u_0)$ . Following the derivation in [BBM17, Chapter 8.2], we substitute out the equality constraints defining the dynamics, and obtain the following **PQP** in the variables  $x = (u_1, \dots, u_{T-1}) \in \mathbf{R}^{2(T-1)}$ ,

$$\begin{aligned}
& \text{minimize} && (1/2)x^T Px \\
& \text{subject to} && l(\theta) \leq Ax \leq u(\theta).
\end{aligned} \tag{32}$$

The output reference cost and input costs enter into the objective through  $P \in \mathbf{S}_{++}^{2(T-1)}$ , and the linear dynamics and input constraints enter in through the constraint matrix  $A \in \mathbf{R}^{4(T-1) \times 2(T-1)}$  and the bounds,  $l(\theta)$  and  $u(\theta)$ . We solve this problem using the **alternating direction method of multipliers (ADMM)** in the form adopted in the **operator splitting quadratic programming (OSQP)** solver [SBG<sup>+</sup>20] without over-relaxation. In Algorithm 5, we write the steps as a fixed-point iterations over iterate  $z^k = (x^k, v^k)$  [BGSB19, Section 4.1], where  $v^k$  implicitly represents dual and slack variables. We use  $\Pi_{\mathcal{C}}(v)$  to denote the projection of a vector  $v \in \mathbf{R}^m$  onto the set  $[l(\theta), u(\theta)]$ , which we outline in Table 1.

---

**Algorithm 5** OSQP algorithm without over-relaxation for a **QP** (32).

---

- 1: **Given** parameters  $\sigma > 0$ , either  $\rho > 0$  OR  $\rho \in \mathbf{S}_{++}$  a diagonal matrix, initial iterate  $z^0 = (x^0, v^0)$ , and  $\mathcal{C} = [l(\theta), u(\theta)]$
  - 2: **for**  $k = 0, \dots, K - 1$  **do**
  - 3:      $w^{k+1} = \Pi_{\mathcal{C}}(v^k)$
  - 4:     Solve  $(P + \sigma I + A^T \rho A)x^{k+1} = \sigma x^k + A^T \rho(2w^{k+1} - v^k)$
  - 5:      $v^{k+1} = \rho Ax^{k+1} + (I + \rho I)v^k - (2\rho I + I)w^{k+1}$
  - 6: **return**  $z^K = (x^K, v^K)$ .
- 

While **OSQP** adapts the step size  $\rho$  throughout iterations [SBG<sup>+</sup>20, Section 5.2], we use a fixed step size  $\rho$  for simplicity. We study two alternatives for  $\rho$ , scalar and diagonal. The scalar  $\rho > 0$  is a single value commonly used in **ADMM**[BPC<sup>+</sup>11]. The diagonal  $\rho$  is a diagonal matrix in  $\mathbf{S}_{++}^{4(T-1)}$  with different step sizes for each index. To improve convergence [SBG<sup>+</sup>20, Section 5.2], we set the same large value step size for the indices where  $l_i(\theta) = u_i(\theta)$  (equality constraints), and the same low value for the other constraints. For the optimal control formulation (32), the first 4 indices have  $l_i(\theta) = u_i(\theta)$ .

**Problem setup.** We choose  $h = 0.1, \eta = 0.1, m = 1, \gamma = 0.2, u^{\max} = 2, d^{\max} = 0.2, T = 5$ . The reference position is the origin,  $y^{\text{ref}} = 0$ . To generate the parametric sets, we simulate the model in a closed loop with noise for  $T_{\text{sim}} = 25$  steps. We start with the vehicle with initial state  $\bar{s} = (5, 5, 0, 0)$  and previous input as  $u_0 = (0, 0)$ , *i.e.*, initial position  $(5, 5)$  at rest and with no previous input force. To generate the parameter sets, we solve the optimal control problem from the initial state, propagate the dynamics forward, and add a noise perturbation each time to compute the successive state  $s_{t+1}$ . The noise is sampled from a Gaussian distribution with mean 0 and standard deviation  $10^{-3}$ . We use  $\theta = (s_{t+1}, u_t)$  to set the parameters for the subsequent optimal control instance. We propagate the dynamics forward with noise for  $T_{\text{sim}}$  steps and save all the state and input values. After repeating the entire simulation  $N$  times, we find the smallest hypercube that contain all values of  $\bar{s}$  and  $u_0$ , obtaining the parameter set  $\Theta$ . In practice, we repeatedly solve optimal control problems with slight parameter variations  $\theta$ . Therefore, a reasonable warm-start value for  $x^0$  is to propagate the dynamics forward one step and shift the control input accordingly [MT21, Section IV][BBM17]. After computing this warm-start value for every sample, we fit the smallest hypercube containing all values of  $(x^0, \rho Ax^0)$  to construct the initial iterate set  $Z$  where iterates  $z = (x, v)$  live. In the OSQP algorithm (5), we fix  $\sigma = 10^{-6}$ . First, we analyze the scalar  $\rho = 1$  case. Second, we consider the diagonal  $\rho$  case where  $\rho_{ii} = 10$  for  $i = 1, \dots, 4$  and 1 otherwise.

**Results.** The results are presented in Figure 12 and Table 11. The diagonal  $\rho$  case has a higher fixed-point residual at  $K = 2$ , but this is expected due to the large  $\rho$  value corresponding to the equality constraints. For higher values of  $K$ , the diagonal  $\rho$  shows better convergence properties. Note that PEP cannot distinguish between the scalar and diagonal  $\rho$  case because of the dimension-free property discussed in Section 3. Since we cannot encode the specific indices of the diagonal  $\rho$  matrix into a PEP SDP, we only include the PEP comparison in the scalar  $\rho$  case. This highlights an advantage of our verification problem framework; it allows us to encode strategies used in modern solvers, such as constraint-dependent step sizes, and analyze their performance.

## 6 Conclusion

We presented a framework for verifying the performance of first-order methods in parametric quadratic optimization, by evaluating the worst-case fixed-point residual after a predetermined number of iterations. We built a collection of common proximal algorithm steps as combinations of two *primitive steps*: affine and element-wise maximum steps. Our framework can explicitly quantify the effects of warm-starting, commonly used in parametric optimization, by directly representing sets for initial iterates and parameters. We established that, in general, solving the PQP verification problem is  $\mathcal{NP}$ -hard, and we constructed strong SDP relaxations via constraint propagation and bound tightening techniques. Using a variety of examples, we showed the flexibility of our framework, and its ability to uncover practical convergence behavior that cannot be captured using standard worst-case analysis techniques.

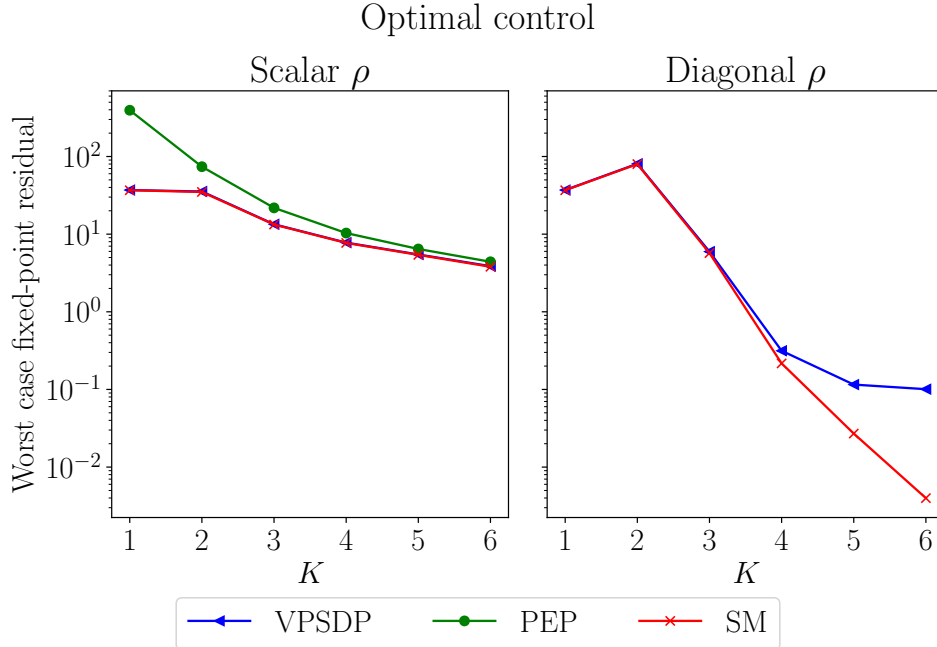


Figure 12: We show the experimental results for the optimal control problem with the OSQP algorithm for Scalar vs. Diagonal  $\rho$  values. Beyond  $K = 2$ , the Diagonal  $\rho$  case outperforms the Scalar  $\rho$  case. We cannot analyze the Diagonal  $\rho$  case via PEP due to its dimension-free property.

To the authors’ knowledge, this is the first work to highlight the potential conservatism of performance estimation approaches in parametric optimization. While our analysis was related to PQPs, we believe that it motivates similar studies for other algorithms targeting parametric convex optimization problems. The main limitations of the proposed approach are that the SDP relaxation cannot easily scale to larger PQP instances, and that the tightness degrades as the number of algorithm steps increases. Future works could address these issues by developing customized solution algorithms to solve large-scale semidefinite relaxations [YTF<sup>+</sup>21], by adopting more scalable alternatives to SDP relaxations [AM19], or by attempting to directly solve a nonconvex formulation of the verification problem [BM03].

## Acknowledgements

The authors are supported by the NSF CAREER Award ECCS-2239771 and the Princeton School of Engineering and Applied Science Innovation grant. The authors are pleased to acknowledge that the work reported on in this paper was substantially performed using the Princeton Research Computing resources at Princeton University which is consortium of groups led by the Princeton Institute for Computational Science and Engineering (PICSciE) and Office of Information Technology’s Research Computing.

## References

- [ADH<sup>+</sup>21] D. Applegate, M. Diaz, O. Hinder, H. Lu, M. Lubin, B. O’Donoghue, and W. Schudy. Practical large-scale linear programming using primal-dual hybrid gradient. *Advances in Neural Information Processing Systems*, 34:20243–20257, 2021.
- [Alb21] A. Albarghouthi. Introduction to neural network verification. *Foundations and Trends in Programming Languages*, 7(1–2):1–157, 2021.
- [AM19] A. A. Ahmadi and A. Majumdar. DSOS and SDSOS optimization: More tractable alternatives to sum of squares and semidefinite optimization. *SIAM Journal on Applied Algebra and Geometry*, 3(2):193–230, 2019.
- [Amo23] B. Amos. Tutorial on amortized optimization. *Foundations and Trends in Machine Learning*, 16(5):592–732, 2023.
- [Ans09] K. Anstreicher. Semidefinite programming versus the reformulation-linearization technique for nonconvex quadratically constrained quadratic programming. *Journal of Global Optimization*, 43:471–484, 2009.
- [AP23a] J. Altschuler and P. Parrilo. Acceleration by stepsize hedging i: Multi-step descent and the silver stepsize schedule. *arXiv:2309.07879*, 2023.
- [AP23b] J. Altschuler and P. Parrilo. Acceleration by stepsize hedging ii: Silver stepsize schedule for smooth convex optimization. *arXiv:2309.16530*, 2023.
- [ApS24] MOSEK ApS. *The MOSEK optimization software.*, 2024.
- [AVDB18] A. Agrawal, R. Verschueren, S. Diamond, and S. Boyd. A rewriting system for convex optimization problems. *Journal of Control and Decision*, 5(1):42–60, 2018.
- [BBM17] F. Borrelli, A. Bemporad, and M. Morari. *Predictive Control for Linear and Hybrid Systems*. Cambridge University Press, 2017.
- [BC17] H. H. Bauschke and P. L. Combettes. *Convex Analysis and Monotone Operator Theory in Hilbert Spaces*. Springer International Publishing, 2017.
- [Bec17] A. Beck. *First-Order Methods in Optimization*. Society for Industrial and Applied Mathematics, Philadelphia, PA, 2017.
- [BGSB19] G. Banjac, P. Goulart, B. Stellato, and S. Boyd. Infeasibility detection in the alternating direction method of multipliers for convex optimization. *Journal of Optimization Theory and Applications*, 183(2):490–519, 2019.

- [BHG22] N. Bousselmi, J. Hendrickx, and F. Glineur. Performance estimation of first-order methods on quadratic functions. *25th International Symposium on Mathematical Theory of Networks and Systems*, 2022.
- [BHG23] N. Bousselmi, J. Hendrickx, and F. Glineur. Interpolation conditions for linear operators and applications to performance estimation problems. *arXiv:2302.08781*, 2023.
- [BLT<sup>+</sup>20] R. Bunel, J. Lu, I. Turkaslan, P. H. S. Torr, P. Kohli, and M. P. Kumar. Branch and bound for piecewise linear neural network verification. *Journal of Machine Learning Research*, 21(42):1–39, 2020.
- [BM03] S. Burer and R. D.C. Monteiro. A nonlinear programming algorithm for solving semidefinite programs via low-rank factorization. *Mathematical programming*, 95(2):329–357, 2003.
- [BMOW14] S. Boyd, M. Mueller, B. O’Donoghue, and Y. Wang. Performance bounds and suboptimal policies for multi-period investment. *Found. Trends Optim.*, 1(1):1–72, 2014.
- [BPC<sup>+</sup>11] S. Boyd, N. Parikh, E. Chu, B. Peleato, and J. Eckstein. Distributed optimization and statistical learning via the alternating direction method of multipliers. *Foundations and Trends in Machine Learning*, 3(1):1–122, 2011.
- [BSAP22] R. Brown, E. Schmerling, N. Azizan, and M. Pavone. A unified view of SDP-based neural network verification through completely positive programming. In *International Conference on Artificial Intelligence and Statistics*, 2022.
- [BT09] A. Beck and M. Teboulle. A fast iterative shrinkage-thresholding algorithm for linear inverse problems. *SIAM Journal on Imaging Sciences*, 2(1):183–202, 2009.
- [BV04] S. Boyd and L. Vandenberghe. *Convex optimization*. Cambridge University Press, 2004.
- [BV18] S. Boyd and L. Vandenberghe. *Introduction to Applied Linear Algebra – Vectors, Matrices, and Least Squares*. Cambridge University Press, 2018.
- [CCC<sup>+</sup>22] T. Chen, X. Chen, W. Chen, H. Heaton, J. Liu, Z. Wang, and W. Yin. Learning to optimize: A primer and a benchmark. *Journal of Machine Learning Research*, 23(189):1–59, 2022.
- [CH23] S. Colla and J. M. Hendrickx. Automatic performance estimation for decentralized optimization. *IEEE Transactions on Automatic Control*, 68(12):7136–7150, 2023.

- [CV95] C. Cortes and V. Vapnik. Support-vector networks. *Machine Learning*, 20(3):273–297, 1995.
- [CWB07] E. Candès, M. Wakin, and S. Boyd. Enhancing sparsity by reweighted l1 minimization. *Journal of Fourier Analysis and Applications*, 14:877–905, 11 2007.
- [CWKF22] S. Chen, E. Wong, J. Z. Kolter, and M. Fazlyab. DeepSplit: Scalable verification of deep neural networks via operator splitting. *IEEE Open Journal of Control Systems*, 1:126–140, 2022.
- [DB16] S. Diamond and S. Boyd. CVXPY: A Python-embedded modeling language for convex optimization. *Journal of Machine Learning Research*, 17(83):1–5, 2016.
- [DDK<sup>+</sup>20] S. Dathathri, K. Dvijotham, A. Kurakin, A. Raghunathan, J. Uesato, R. R. Bunel, S. Shankar, J. Steinhardt, I. Goodfellow, P. S. Liang, and P. Kohli. Enabling certification of verification-agnostic networks via memory-efficient semidefinite programming. *Advances in Neural Information Processing Systems*, 33:5318–5331, 2020.
- [DGVPR23] S. Das Gupta, B. Van Parys, and E. Ryu. Branch-and-bound performance estimation programming: a unified methodology for constructing optimal optimization methods. *Mathematical Programming*, pages 1–73, 2023.
- [DR56] J. Douglas and H. Rachford. On the numerical solution of heat conduction problems in two and three space variables. *Transactions of the American Mathematical Society*, 82:421–439, 1956.
- [DT14] Y. Drori and M. Teboulle. Performance of first-order methods for smooth convex minimization: a novel approach. *Math. Program.*, 145(1-2):451–482, 2014.
- [Ehl17] R. Ehlers. Formal verification of piece-wise linear feed-forward neural networks. *Automated Technology for Verification and Analysis*, pages 269–286, 2017.
- [FJ18] M. Fischetti and J. Jo. Deep neural networks and mixed integer linear optimization. *Constraints*, 23(3):296—309, jul 2018.
- [FMP22] M. Fazlyab, M. Morari, and G. J. Pappas. Safety verification and robustness analysis of neural networks via quadratic constraints and semidefinite programming. *IEEE Transactions on Automatic Control*, 67(1):1–15, 2022.
- [FW56] M. Frank and P. Wolfe. An algorithm for quadratic programming. *Naval Research Logistics Quarterly*, 8(2):604–616, 1956.
- [GDS<sup>+</sup>18] S. Gowal, K. Dvijotham, R. Stanforth, R. Bunel, C. Qin, J. Uesato, R. Arandjelović, T. Mann, and P. Kohli. On the effectiveness of interval bound propagation for training verifiably robust models. *arXiv:1810.12715*, 2018.

- [GM76] D. Gabay and B. Mercier. A dual algorithm for the solution of nonlinear variational problems via finite element approximation. *Computers & Mathematics with Applications*, 2(1):17–40, 1976.
- [GMG<sup>+</sup>22] B. Goujaud, C. Moucer, F. Glineur, J. Hendrickx, A. Taylor, and A. Dieuleveut. PEPit: computer-assisted worst-case analyses of first-order optimization methods in Python. *arXiv preprint arXiv:2201.04040*, 2022.
- [Gur22] Gurobi Optimization, LLC. Gurobi Optimizer Reference Manual, 2022.
- [HL17] B. Hu and L. Lessard. Dissipativity theory for Nesterov’s accelerated method. In *International Conference on Machine Learning*, pages 1549–1557. PMLR, 2017.
- [Hub64] P. Huber. Robust Estimation of a Location Parameter. *The Annals of Mathematical Statistics*, 35(1):73 – 101, 1964.
- [JDGR23] U. Jang, S. Das Gupta, and E. Ryu. Computer-assisted design of accelerated composite optimization methods: OptISTA. *arXiv:2305.15704*, 2023.
- [JGR<sup>+</sup>14] J. L. Jerez, P. J. Goulart, S. Richter, G. A. Constantinides, E. C. Kerrigan, and M. Morari. Embedded online optimization for model predictive control at megahertz rates. *IEEE Transactions on Automatic Control*, 59(12):3238–3251, 12 2014.
- [JL20] R. Jiang and D. Li. Semidefinite programming based convex relaxation for nonconvex quadratically constrained quadratic programming. In *Optimization of Complex Systems: Theory, Models, Algorithms and Applications*, pages 213–220. Springer International Publishing, 2020.
- [Kar72] R. Karp. Reducibility among combinatorial problems. *Complexity of Computer Computations*, pages 85–103, 1972.
- [LAL<sup>+</sup>21] C. Liu, T. Arnon, C. Lazarus, C. Strong, C. Barrett, and M. J. Kochenderfer. Algorithms for verifying deep neural networks. *Foundations and Trends in Optimization*, 4(3-4):244–404, 2021.
- [LRP16] L. Lessard, B. Recht, and A. Packard. Analysis and design of optimization algorithms via integral quadratic constraints. *SIAM Journal on Optimization*, 26(1):57–95, jan 2016.
- [Mar52] H. Markowitz. Portfolio selection. *The Journal of Finance*, 7(1):77–91, 1952.
- [MB10a] J. Mattingley and S. Boyd. Automatic code generation for real-time convex optimization. *Convex optimization in signal processing and communications*, 01 2010.

- [MB10b] J. Mattingley and S. Boyd. Real-time convex optimization in signal processing. *IEEE Signal Processing Magazine*, 27(3):50–61, May 2010.
- [McA98] D. McAllester. Some pac-bayesian theorems. In *Proceedings of the Eleventh Annual Conference on Computational Learning Theory*, COLT’ 98, page 230–234, New York, NY, USA, 1998. Association for Computing Machinery.
- [MT21] T. Marcucci and R. Tedrake. Warm start of mixed-integer programs for model predictive control of hybrid systems. *IEEE Transactions on Automatic Control*, 66(6):2433–2448, June 2021.
- [Nes83] Y. Nesterov. A method for solving the convex programming problem with convergence rate  $o(1/k^2)$ . *Proceedings of the USSR Academy of Sciences*, 269:543–547, 1983.
- [Nes18] Y. Nesterov. *Lectures on Convex Optimization*. Springer Optimization and Its Applications. Springer International Publishing, 2018.
- [NP21] M. Newton and A. Papachristodoulou. Exploiting sparsity for neural network verification. In *Proceedings of the 3rd Conference on Learning for Dynamics and Control*, volume 144 of *Proceedings of Machine Learning Research*, pages 715–727. PMLR, 08 2021.
- [OCPB16] B. O’Donoghue, E. Chu, N. Parikh, and S. Boyd. Conic optimization via operator splitting and homogeneous self-dual embedding. *Journal of Optimization Theory and Applications*, 169(3):1042–1068, 6 2016.
- [O’D21] B. O’Donoghue. Operator splitting for a homogeneous embedding of the linear complementarity problem. *SIAM Journal on Optimization*, 31(3):1999–2023, 2021.
- [OSB13] B. O’Donoghue, G. Stathopoulos, and S. Boyd. A splitting method for optimal control. *IEEE Transactions on Control Systems Technology*, 21(6):2432–2442, 11 2013.
- [PB13] N. Parikh and S. Boyd. Proximal algorithms. *Foundations and Trends in Optimization*, 1(3):123–231, 2013.
- [PB17] J. Park and S. Boyd. General heuristics for nonconvex quadratically constrained quadratic programming. *arXiv:1703.07870*, 2017.
- [PT07] I. Pólik and T. Terlaky. A survey of the s-lemma. *SIAM Review*, 49(3):371–418, 2007.
- [RB16] E. Ryu and S. Boyd. A primer on monotone operator methods survey. *Applied and computational mathematics*, 15:3–43, 01 2016.

- [RJM12] S. Richter, C. N. Jones, and M. Morari. Computational complexity certification for real-time mpc with input constraints based on the fast gradient method. *IEEE Transactions on Automatic Control*, 57(6):1391–1403, 2012.
- [RM09] J. Rawlings and D. Mayne. *Model Predictive Control: Theory and Design*. Nob Hill Pub., 2009.
- [RSL18] A. Raghunathan, J. Steinhardt, and P. S. Liang. Semidefinite relaxations for certifying robustness to adversarial examples. *Advances in Neural Information Processing Systems*, 31, 2018.
- [RTBG20] E. Ryu, A. Taylor, C. Bergeling, and P. Giselsson. Operator splitting performance estimation: Tight contraction factors and optimal parameter selection. *SIAM Journal on Optimization*, 30(3):2251–2271, 2020.
- [RY22] E. Ryu and W. Yin. *Large-Scale Convex Optimization*. Cambridge University Press, 11 2022.
- [SA10] H. Serali and W. Adams. *A Reformulation-Linearization Technique for Solving Discrete and Continuous Nonconvex Problems*, volume 31. Springer New York, NY, 01 2010.
- [SBG<sup>+</sup>20] B. Stellato, G. Banjac, P. Goulart, A. Bemporad, and S. Boyd. OSQP: an operator splitting solver for quadratic programs. *Mathematical Programming Computation*, 12(4):637–672, 2020.
- [SHAS22] R. Sambharya, G. Hall, B. Amos, and B. Stellato. End-to-End Learning to Warm-Start for Real-Time Quadratic Optimization. *arXiv e-prints*, 12 2022.
- [SHAS23] R. Sambharya, G. Hall, B. Amos, and B. Stellato. Learning to warm-start fixed-point optimization algorithms. *arXiv preprint arXiv:2309.07835*, 2023.
- [SSS<sup>+</sup>16] G. Stathopoulos, H. Shukla, A. Szucs, Y. Pu, and C. N. Jones. Operator splitting methods in control. *Foundations and Trends in Systems and Control*, 3(3):249–362, 2016.
- [STW97] J. Shawe-Taylor and R. Williamson. A pac analysis of a bayesian estimator. In *Proceedings of the Tenth Annual Conference on Computational Learning Theory*, COLT '97, page 2–9, New York, NY, USA, 1997. Association for Computing Machinery.
- [THG17a] A. Taylor, J. Hendrickx, and F. Glineur. Exact worst-case performance of first-order methods for composite convex optimization. *SIAM J. Optim.*, 27(3):1283–1313, 2017.

- [THG17b] A. Taylor, J. Hendrickx, and F. Glineur. Performance estimation toolbox (PESTO): Automated worst-case analysis of first-order optimization methods. In *2017 IEEE 56th Annual Conference on Decision and Control (CDC)*, pages 1278–1283, 2017.
- [THG17c] A. Taylor, J. Hendrickx, and F. Glineur. Smooth strongly convex interpolation and exact worst-case performance of first-order methods. *Math. Program.*, 161(1-2):307–345, 2017.
- [Tib96] R. Tibshirani. Regression shrinkage and selection via the lasso. *Journal of the Royal Statistical Society: Series B*, 58(1):267–288, 1996.
- [TVSL18] A. Taylor, B. Van Scoy, and L. Lessard. Lyapunov functions for first-order methods: Tight automated convergence guarantees. In *Proceedings of the 35th International Conference on Machine Learning*, volume 80 of *Proceedings of Machine Learning Research*, pages 4897–4906. PMLR, 10–15 Jul 2018.
- [TXT19] V. Tjeng, K. Y. Xiao, and R. Tedrake. Evaluating robustness of neural networks with mixed integer programming. In *International Conference on Learning Representations*, 2019.
- [WKK21] A. Wang and F. Kılınç-Karzan. On the tightness of sdp relaxations of qcqps. *Mathematical Programming*, 193, 01 2021.
- [WZX<sup>+</sup>21] S. Wang, H. Zhang, K. Xu, X. Lin, S. Jana, C. Hsieh, and Z. Kolter. Beta-CROWN: Efficient bound propagation with per-neuron split constraints for complete and incomplete neural network verification. *Advances in Neural Information Processing Systems*, 34, 2021.
- [XSZ<sup>+</sup>20] K. Xu, Z. Shi, H. Zhang, Y. Wang, K.-W. Chang, M. Huang, B. Kailkhura, X. Lin, and C.-J. Hsieh. Automatic perturbation analysis for scalable certified robustness and beyond. *Advances in Neural Information Processing Systems*, 33, 2020.
- [XZW<sup>+</sup>21] K. Xu, H. Zhang, S. Wang, Y. Wang, S. Jana, X. Lin, and C. Hsieh. Fast and Complete: Enabling complete neural network verification with rapid and massively parallel incomplete verifiers. In *International Conference on Learning Representations*, 2021.
- [Yak71] V. Yakubovich. S-procedure in nonlinear control theory. *Vestnik Leningrad. Univ. (in Russian)*, 4:62–77, 1971.
- [YTF<sup>+</sup>21] A. Yurtsever, J. A. Tropp, O. Fercoq, M. Udell, and V. Cevher. Scalable semidefinite programming. *SIAM Journal on Mathematics of Data Science*, 3(1):171–200, 2021.

- [ZFP<sup>+</sup>17] Y. Zheng, G. Fantuzzi, A. Papachristodoulou, P. Goulart, and A. Wynn. Fast admm for semidefinite programs with chordal sparsity. 05 2017.
- [ZFP21] Y. Zheng, G. Fantuzzi, and A. Papachristodoulou. Chordal and factor-width decompositions for scalable semidefinite and polynomial optimization. *Annual Reviews in Control*, 52:243–279, 2021.
- [ZWC<sup>+</sup>18] H. Zhang, T.-W. Weng, P.-Y. Chen, C.-J. Hsieh, and L. Daniel. Efficient neural network robustness certification with general activation functions. *Advances in Neural Information Processing Systems*, 31:4939–4948, 2018.
- [ZWX<sup>+</sup>22a] H. Zhang, S. Wang, K. Xu, L. Li, B. Li, S. Jana, C. Hsieh, and Z. Kolter. General cutting planes for bound-propagation-based neural network verification. *Advances in Neural Information Processing Systems*, 2022.
- [ZWX<sup>+</sup>22b] H. Zhang, S. Wang, K. Xu, Y. Wang, S. Jana, C. Hsieh, and Z. Kolter. A branch and bound framework for stronger adversarial attacks of ReLU networks. In *Proceedings of the 39th International Conference on Machine Learning*, volume 162, pages 26591–26604, 2022.

## A Proof of Proposition 3.1

From [BV04, Chapter 9][Nes18, Chapter 2], for any  $L$ -smooth and  $\mu$ -strongly convex function, we have that

$$\|z^k - z^*\| \leq \tau \|z^{k-1} - z^*\|, \tag{33}$$

where  $\tau = \max\{|1 - t\mu|, |1 - tL|\}$ . For  $t \in (0, 2/L)$ , we have that  $\tau \in (0, 1)$ , so the gradient step is contractive. To instead analyze the fixed-point residual, we apply the triangle inequality:

$$\begin{aligned} \|z^k - z^{k-1}\| &\leq \|z^k - z^*\| + \|z^{k-1} - z^*\| \\ &\leq (1 + \tau) \|z^{k-1} - z^*\| \\ &\leq \tau^{k-1} (1 + \tau) \|z^0 - z^*\|. \end{aligned}$$

For any  $k$ , the expression  $\tau^{k-1}(1 + \tau)$  is increasing for positive  $\tau$  since the derivative is positive. Since  $\tau$  is minimized at  $t = 2/(\mu + L)$  [Nes18, Equation 1.2.27] and  $\tau > 0$ , the right hand side coefficient is minimized for the same  $t$  value as well.

## B Proofs for Section 4

### B.1 Proof of Theorem 4.1

We show problem (VP) is  $\mathcal{NP}$ -hard via a reduction from the 0-1 integer programming feasibility problem. Specifically, deciding if there exists a feasible solution to the following

integer program:

$$\begin{aligned}
& \text{minimize} && 0 \\
& \text{subject to} && Ax = b, \\
& && x \in \{0, 1\}^n,
\end{aligned} \tag{34}$$

is an  $\mathcal{NP}$ -hard problem [Kar72, Section 4]. Consider the following related optimization problem:

$$\begin{aligned}
& \text{maximize} && \|x - (1/2)\mathbf{1}\|^2 \\
& \text{subject to} && Ax = b, \\
& && 0 \leq x \leq 1.
\end{aligned} \tag{35}$$

Note that the integrality constraints from (34) were relaxed to be continuous in (35). We have  $\|x - (1/2)\mathbf{1}\|^2 = \sum_{i=1}^n (x_i - 1/2)^2$ , and on  $0 \leq x_i \leq 1$ ,  $(x_i - 1/2)^2$  is maximized at  $x_i = 0$  or  $x_i = 1$  with value  $1/4$ . Since  $(x_i - 1/2)^2 \geq 0$ , the optimal value of (35) is  $n/4$  if and only if (34) is feasible. So, it is  $\mathcal{NP}$ -hard to determine if the optimal value of (35) is  $n/4$ . We can rewrite (35) as

$$\begin{aligned}
& \text{maximize} && \|y^1 - y^0\|^2 \\
& \text{subject to} && y^1 = x^0 - (1/2)q(\theta), \\
& && y^0 = 0, \\
& && q(\theta) = \mathbf{1}, \\
& && Ax^0 = b, \\
& && 0 \leq x^0 \leq 1.
\end{aligned} \tag{36}$$

Every constraint in (36) is either an affine step, a box constraint, or a polyhedral constraint. So, we have reduced the 0-1 integer feasibility problem to deciding the maximum value of a verification problem, which proves that finding the optimal value of the verification problem is  $\mathcal{NP}$ -hard.

## B.2 Proof of Proposition 4.1

We first introduce a helper lemma about traces and matrix products.

**Lemma B.1** (trace of positive semidefinite matrix product). *If  $A, B \in \mathbf{S}_+^{d \times d}$  are positive semidefinite, then  $\text{tr}(AB) \geq 0$ .*

*Proof.* Since  $B$  is positive semidefinite, it has a square root, *i.e.* a positive semidefinite matrix  $H \in \mathbf{S}_+^{d \times d}$  such that  $B = HH^T$ . Applying the cyclic property of the trace gives

$$\text{tr}(AB) = \text{tr}(AHH^T) = \text{tr}(H^T AH).$$

For any  $x$ , since  $A$  is also positive semidefinite,

$$x^T H^T AH x = (Hx)^T A(Hx) \geq 0.$$

This proves  $H^T AH$  is positive semidefinite, therefore  $\text{tr}(H^T AH) \geq 0$ . ■

We can now proceed in proving Proposition 4.1. By rewriting  $f(x, y)$  and applying the cyclic property of the trace, we have:

$$\|x - y\|^2 = \begin{bmatrix} x \\ y \end{bmatrix}^T \begin{bmatrix} I & -I \\ -I & I \end{bmatrix} \begin{bmatrix} x \\ y \end{bmatrix} = \mathbf{tr} \left( \begin{bmatrix} I & -I \\ -I & I \end{bmatrix} \begin{bmatrix} x \\ y \end{bmatrix} \begin{bmatrix} x \\ y \end{bmatrix}^T \right).$$

We choose

$$M = \begin{bmatrix} x \\ y \end{bmatrix} \begin{bmatrix} x \\ y \end{bmatrix}^T,$$

relax the equality to inequality, and apply the Schur complement, similar to the derivation in (14).

Since the squared norm is a convex function and the difference  $x - y$  is affine, the entire expression is convex and, therefore, the coefficient matrix inside the trace is positive semidefinite. This allows us to apply Lemma B.1 and finish the proof.

### B.3 Proof of Proposition 4.2

Since  $D$  is assumed to be invertible,  $F$  is nonempty for any  $A, B, D$ . Given  $(y, x, q) \in F$ , observe that

$$(Dy)(Dy)^T = (Ax + Bq)(Ax + Bq)^T \implies Dyy^T D^T = \begin{bmatrix} A & B \end{bmatrix} \begin{bmatrix} x \\ q \end{bmatrix} \begin{bmatrix} x \\ q \end{bmatrix}^T \begin{bmatrix} A^T \\ B^T \end{bmatrix}.$$

We finish the proof by choosing

$$M_1 = yy^T, \quad M_2 = \begin{bmatrix} x \\ q \end{bmatrix} \begin{bmatrix} x \\ q \end{bmatrix}^T,$$

relaxing the equalities to inequalities, and applying the Schur complement to each.

### B.4 Proof of Proposition 4.3

Similar to our proof of Proposition 4.2, given  $(y, x, l) \in F$ , recall from Section 2.1 that

$$y = \max\{x, l\} \iff y \geq x, \quad y \geq l, \quad (y - l)^T(y - x) = 0.$$

The complementarity constraint requires cyclic property of the trace:

$$\begin{aligned} (y - l)^T(y - x) &= \begin{bmatrix} y \\ x \\ l \end{bmatrix}^T \begin{bmatrix} I & -I/2 & -I/2 \\ -I/2 & 0 & I/2 \\ -I/2 & I/2 & 0 \end{bmatrix} \begin{bmatrix} y \\ x \\ l \end{bmatrix} \\ &= \mathbf{tr} \left( \begin{bmatrix} I & -I/2 & -I/2 \\ -I/2 & 0 & I/2 \\ -I/2 & I/2 & 0 \end{bmatrix} \begin{bmatrix} y \\ x \\ l \end{bmatrix} \begin{bmatrix} y \\ x \\ l \end{bmatrix}^T \right) = 0. \end{aligned}$$

We choose

$$M = \begin{bmatrix} y \\ x \\ l \end{bmatrix} \begin{bmatrix} y \\ x \\ l \end{bmatrix}^T,$$

and finish the proof by relaxing the equality to inequality and applying the Schur complement.

## B.5 Proof of Proposition 4.4

The bounds  $l \leq z \leq u$  can be rewritten as  $u - z \geq 0$ ,  $z - l \geq 0$ . By cross-multiplying the lower and upper bound inequalities, we derive:

$$(u - z)(z - l)^T = uz^T - ul^T - zz^T + zl^T \geq 0.$$

We choose  $M = zz^T$ , relax the equality to inequality, and apply the Schur complement to finish the proof.

## B.6 Proof of Proposition 4.5

We introduce a slack variable so the polyhedral constraints can be represented as:

$$Az + s = b, \quad s \geq 0.$$

We relax the constraints in a similar way to our proof in Proposition 4.2. Specifically, we multiply the equality constraints with themselves:

$$(Az + s)(Az + s)^T = \begin{bmatrix} A & I \end{bmatrix} \begin{bmatrix} z \\ s \end{bmatrix} \begin{bmatrix} z \\ s \end{bmatrix}^T \begin{bmatrix} A \\ I \end{bmatrix} = bb^T.$$

We finish the proof by choosing

$$M = \begin{bmatrix} z \\ s \end{bmatrix} \begin{bmatrix} z \\ s \end{bmatrix}^T.$$

We relax the equalities to inequalities and apply the Schur complement.

## B.7 Proof of Proposition 4.6

Squaring the constraint in  $F$  gives

$$z^T z - 2z^T c + c^T c \leq r^2.$$

Applying the cyclic property of the trace gives:

$$z^T z - 2z^T c + c^T c = \begin{bmatrix} z \\ c \end{bmatrix}^T \begin{bmatrix} I & -I \\ -I & I \end{bmatrix} \begin{bmatrix} z \\ c \end{bmatrix} = \mathbf{tr} \left( \begin{bmatrix} I & -I \\ -I & I \end{bmatrix} \begin{bmatrix} z \\ c \end{bmatrix} \begin{bmatrix} z \\ c \end{bmatrix}^T \right).$$

We choose

$$M = \begin{bmatrix} z \\ c \end{bmatrix} \begin{bmatrix} z \\ c \end{bmatrix}^T,$$

relax the equality and apply the Schur complement to finish the proof.

## C Maintaining SDP coupling

From the derivations in Section 4.3, we have multiple matrix variables with corresponding positive semidefinite constraints. As shown in the end of Section 4.5, when matrix variables contain shared submatrices, we can reuse parts of the matrix variables for multiple sets of constraints. We can extend this idea by considering all block matrices that correspond to shared iterates or parameters in the verification problem. For an illustrative example, consider two gradient steps with a nonnegative orthant projection between:

$$\begin{aligned} y^{k+1} &= (I - tP)z^k - tq(\theta) \\ z^{k+1} &= (y^{k+1})_+ \\ y^{k+2} &= (I - tP)z^{k+1} - tq(\theta), \end{aligned}$$

which, using Propositions 4.2 and 4.3, leads to the following matrix variables:

$$\begin{aligned} &\begin{bmatrix} M_1 & y^{k+1} \\ (y^{k+1})^T & 1 \end{bmatrix}, \quad \begin{bmatrix} M_2 & z^k \\ (z^k)^T & q(\theta) \\ q(\theta)^T & 1 \end{bmatrix}, \quad \begin{bmatrix} M_3 & z^{k+1} \\ (z^{k+1})^T & y^{k+1} \\ (y^{k+1})^T & 1 \end{bmatrix}, \\ &\begin{bmatrix} M_4 & y^{k+2} \\ (y^{k+2})^T & 1 \end{bmatrix}, \quad \begin{bmatrix} M_5 & z^{k+1} \\ (z^{k+1})^T & q(\theta) \\ q(\theta)^T & 1 \end{bmatrix}. \end{aligned}$$

We require each of these matrix variables to be positive semidefinite, and we also require equality between the corresponding components of the different matrix variables. In particular, the upper left  $n \times n$  submatrix of both  $M_3$  and  $M_5$  correspond to the iterate  $z^{k+1}$ . So, to tighten the relaxation, we can impose equality between the upper left submatrices. Additionally, the bottom right submatrix of both  $M_2$  and  $M_5$  correspond to the parameter  $q(\theta)$ . While we only show two steps here, for a full  $K$  step verification problem with gradient steps,  $q(\theta)$  is coupled with at least  $K$  different positive semidefinite constraints.

To enforce equality across all positive semidefinite constraints, we use techniques from the SDP chordal sparsity literature [ZFP21], [ZFP+17, Section III]. Specifically, we introduce consensus variables for the matrix variables and use these to jointly enforce positive semidefiniteness and equality across the matrices. Recall that using the Schur complement means we enforce  $M_1 \succeq y^{k+1}(y^{k+1})^T$ ,  $M_4 \succeq y^{k+2}(y^{k+2})^T$ . For notation, we introduce new consensus variables  $H^k, H^{k+1}, Q$  that correspond to:

$$H^k \succeq z^k(z^k)^T, \quad H^{k+1} \succeq z^{k+1}(z^{k+1})^T, \quad Q \succeq q(\theta)q(\theta)^T. \quad (37)$$

With these variables, we enforce equality with the other matrix variables:

$$M_2 = \begin{bmatrix} H^k & \star \\ \star & Q \end{bmatrix}, \quad M_3 = \begin{bmatrix} H^{k+1} & \star \\ \star & M_1 \end{bmatrix}, \quad M_5 = \begin{bmatrix} H^{k+1} & \star \\ \star & Q \end{bmatrix},$$

where the  $\star$  is just a placeholder for the corresponding submatrices without introducing extra unnecessary notation.

We can also use the consensus variables to reduce the number of positive semidefinite constraints. In our simple example, observe that the equality through the consensus variables implies:

$$\begin{bmatrix} M_3 & z^{k+1} \\ (z^{k+1})^T & y^{k+1} \\ (y^{k+1})^T & 1 \end{bmatrix} \succeq 0 \implies \begin{bmatrix} M_1 & y^{k+1} \\ (y^{k+1})^T & 1 \end{bmatrix} \succeq 0.$$

So, when forming and solving the [SDP](#), we can remove the latter positive semidefinite constraint to reduce the problem dimensionality.

## D Numerical result tables

In this section we provide full data tables for every experiment in [Section 5](#).

Table 2: Nonnegative least squares results, nonstrongly convex case, and step size fixed across  $K$ . Corresponds to Figure 6 (first part).

$t$	$K$	VPSDP	SM	PEP	VPSDP solve time (s)	$\frac{\text{PEP}}{\text{VPSDP}}$	$\frac{\text{PEP}}{\text{SM}}$
0.01	1	$4.40 \times 10^1$	$4.37 \times 10^1$	$3.39 \times 10^2$	$4.72 \times 10^1$	7.71	7.76
	2	$1.33 \times 10^1$	$1.32 \times 10^1$	$8.49 \times 10^1$	$1.01 \times 10^2$	6.37	6.41
	3	5.54	5.50	$3.77 \times 10^1$	$1.63 \times 10^2$	6.81	6.86
	4	2.71	2.69	$2.12 \times 10^1$	$2.50 \times 10^2$	7.83	7.89
	5	1.48	1.47	$1.36 \times 10^1$	$4.42 \times 10^2$	9.19	9.27
	6	$8.69 \times 10^{-1}$	$8.60 \times 10^{-1}$	9.43	$6.84 \times 10^2$	$1.09 \times 10^1$	$1.10 \times 10^1$
	7	$5.35 \times 10^{-1}$	$5.28 \times 10^{-1}$	6.93	$5.15 \times 10^2$	$1.30 \times 10^1$	$1.31 \times 10^1$
	8	$3.41 \times 10^{-1}$	$3.34 \times 10^{-1}$	5.30	$5.09 \times 10^2$	$1.55 \times 10^1$	$1.59 \times 10^1$
	9	$2.38 \times 10^{-1}$	$2.17 \times 10^{-1}$	4.19	$5.97 \times 10^2$	$1.76 \times 10^1$	$1.93 \times 10^1$
	10	$1.73 \times 10^{-1}$	$1.43 \times 10^{-1}$	3.39	$7.65 \times 10^2$	$1.96 \times 10^1$	$2.37 \times 10^1$
0.0125	1	$6.88 \times 10^1$	$6.83 \times 10^1$	$5.30 \times 10^2$	$4.21 \times 10^1$	7.71	7.76
	2	$1.43 \times 10^1$	$1.42 \times 10^1$	$1.05 \times 10^2$	$1.13 \times 10^2$	7.35	7.39
	3	5.30	5.26	$4.33 \times 10^1$	$1.62 \times 10^2$	8.18	8.24
	4	2.38	2.36	$2.35 \times 10^1$	$2.71 \times 10^2$	9.88	9.97
	5	1.21	1.20	$1.47 \times 10^1$	$5.08 \times 10^2$	$1.22 \times 10^1$	$1.23 \times 10^1$
	6	$6.62 \times 10^{-1}$	$6.54 \times 10^{-1}$	$1.01 \times 10^1$	$6.40 \times 10^2$	$1.52 \times 10^1$	$1.54 \times 10^1$
	7	$3.95 \times 10^{-1}$	$3.72 \times 10^{-1}$	7.34	$5.64 \times 10^2$	$1.86 \times 10^1$	$1.97 \times 10^1$
	8	$2.48 \times 10^{-1}$	$2.19 \times 10^{-1}$	5.58	$5.78 \times 10^2$	$2.25 \times 10^1$	$2.55 \times 10^1$
	9	$1.56 \times 10^{-1}$	$1.33 \times 10^{-1}$	4.38	$6.32 \times 10^2$	$2.81 \times 10^1$	$3.31 \times 10^1$
	10	$1.20 \times 10^{-1}$	$8.20 \times 10^{-2}$	3.53	$8.10 \times 10^2$	$2.94 \times 10^1$	$4.31 \times 10^1$
0.015	1	$9.91 \times 10^1$	$9.84 \times 10^1$	$7.64 \times 10^2$	$4.19 \times 10^1$	7.71	7.76
	2	$1.42 \times 10^1$	$1.41 \times 10^1$	$1.91 \times 10^2$	$9.99 \times 10^1$	$1.34 \times 10^1$	$1.35 \times 10^1$
	3	4.88	4.83	$4.77 \times 10^1$	$1.72 \times 10^2$	9.79	9.88
	4	2.02	2.00	$2.53 \times 10^1$	$2.76 \times 10^2$	$1.25 \times 10^1$	$1.26 \times 10^1$
	5	$9.53 \times 10^{-1}$	$9.42 \times 10^{-1}$	$1.56 \times 10^1$	$5.35 \times 10^2$	$1.64 \times 10^1$	$1.65 \times 10^1$
	6	$4.85 \times 10^{-1}$	$4.75 \times 10^{-1}$	$1.06 \times 10^1$	$6.66 \times 10^2$	$2.18 \times 10^1$	$2.22 \times 10^1$
	7	$3.29 \times 10^{-1}$	$2.51 \times 10^{-1}$	7.64	$6.33 \times 10^2$	$2.32 \times 10^1$	$3.04 \times 10^1$
	8	$1.78 \times 10^{-1}$	$1.38 \times 10^{-1}$	5.78	$5.16 \times 10^2$	$3.24 \times 10^1$	$4.18 \times 10^1$
	9	$1.25 \times 10^{-1}$	$7.51 \times 10^{-2}$	4.52	$8.46 \times 10^2$	$3.63 \times 10^1$	$6.02 \times 10^1$
	10	$1.03 \times 10^{-1}$	$3.96 \times 10^{-2}$	3.63	$1.00 \times 10^3$	$3.54 \times 10^1$	$9.17 \times 10^1$

Table 3: Nonnegative least squares results, nonstrongly convex case, and step size fixed across  $K$ . Corresponds to Figure 6 (second part).

$t$	$K$	VPSDP	SM	PEP	VPSDP solve time (s)	$\frac{\text{PEP}}{\text{VPSDP}}$	$\frac{\text{PEP}}{\text{SM}}$
0.0175	1	$1.35 \times 10^2$	$1.34 \times 10^2$	$1.04 \times 10^3$	$4.20 \times 10^1$	7.71	7.76
	2	$1.50 \times 10^1$	$1.49 \times 10^1$	$5.85 \times 10^2$	$1.08 \times 10^2$	$3.89 \times 10^1$	$3.92 \times 10^1$
	3	4.46	4.41	$3.29 \times 10^2$	$1.77 \times 10^2$	$7.38 \times 10^1$	$7.45 \times 10^1$
	4	1.66	1.64	$1.85 \times 10^2$	$2.66 \times 10^2$	$1.12 \times 10^2$	$1.13 \times 10^2$
	5	$7.22 \times 10^{-1}$	$7.10 \times 10^{-1}$	$1.04 \times 10^2$	$5.89 \times 10^2$	$1.44 \times 10^2$	$1.47 \times 10^2$
	6	$3.47 \times 10^{-1}$	$3.32 \times 10^{-1}$	$5.85 \times 10^1$	$4.94 \times 10^2$	$1.69 \times 10^2$	$1.76 \times 10^2$
	7	$1.94 \times 10^{-1}$	$1.64 \times 10^{-1}$	$3.29 \times 10^1$	$6.85 \times 10^2$	$1.70 \times 10^2$	$2.01 \times 10^2$
	8	$1.36 \times 10^{-1}$	$7.55 \times 10^{-2}$	$1.85 \times 10^1$	$6.30 \times 10^2$	$1.36 \times 10^2$	$2.45 \times 10^2$
	9	$9.14 \times 10^{-2}$	$3.83 \times 10^{-2}$	$1.04 \times 10^1$	$9.10 \times 10^2$	$1.14 \times 10^2$	$2.72 \times 10^2$
	10	$1.26 \times 10^{-1}$	$2.10 \times 10^{-2}$	5.86	$1.02 \times 10^3$	$4.67 \times 10^1$	$2.79 \times 10^2$
0.02	1	$1.76 \times 10^2$	$1.75 \times 10^2$	$1.36 \times 10^3$	$4.56 \times 10^1$	7.71	7.76
	2	$1.95 \times 10^1$	$1.93 \times 10^1$	$1.36 \times 10^3$	$1.10 \times 10^2$	$6.97 \times 10^1$	$7.04 \times 10^1$
	3	4.76	4.70	$1.36 \times 10^3$	$1.78 \times 10^2$	$2.85 \times 10^2$	$2.89 \times 10^2$
	4	1.43	1.41	$1.36 \times 10^3$	$2.72 \times 10^2$	$9.51 \times 10^2$	$9.64 \times 10^2$
	5	$5.64 \times 10^{-1}$	$5.38 \times 10^{-1}$	$1.36 \times 10^3$	$4.78 \times 10^2$	$2.41 \times 10^3$	$2.52 \times 10^3$
	6	$2.50 \times 10^{-1}$	$2.31 \times 10^{-1}$	$1.36 \times 10^3$	$5.06 \times 10^2$	$5.42 \times 10^3$	$5.89 \times 10^3$
	7	$1.48 \times 10^{-1}$	$9.44 \times 10^{-2}$	$1.36 \times 10^3$	$7.09 \times 10^2$	$9.17 \times 10^3$	$1.44 \times 10^4$
	8	$1.13 \times 10^{-1}$	$4.37 \times 10^{-2}$	$1.36 \times 10^3$	$6.84 \times 10^2$	$1.20 \times 10^4$	$3.11 \times 10^4$
	9	$2.45 \times 10^{-1}$	$2.27 \times 10^{-2}$	$1.36 \times 10^3$	$9.18 \times 10^2$	$5.55 \times 10^3$	$5.99 \times 10^4$
	10	$2.51 \times 10^{-1}$	$1.28 \times 10^{-2}$	$1.36 \times 10^3$	$1.08 \times 10^3$	$5.40 \times 10^3$	$1.06 \times 10^5$

Table 4: Nonnegative least squares results, nonstrongly convex case, and silver step size schedule. Corresponds to Figure 8.

Schedule	$K$	$t$	VPSDP	SM	PEP	VPSDP solve time (s)	$\frac{\text{PEP}}{\sqrt{\text{VPSDP}}}$	$\frac{\text{PEP}}{\text{SM}}$
Nonstrongly cvx.	1	$1.41 \times 10^{-2}$	$8.81 \times 10^1$	$8.75 \times 10^1$	$6.79 \times 10^2$	$6.80 \times 10^1$	7.71	7.76
	2	$2.00 \times 10^{-2}$	$2.81 \times 10^1$	$2.79 \times 10^1$	$2.99 \times 10^2$	$1.50 \times 10^2$	$1.06 \times 10^1$	$1.07 \times 10^1$
	3	$1.41 \times 10^{-2}$	3.01	2.97	$1.47 \times 10^2$	$2.67 \times 10^2$	$4.87 \times 10^1$	$4.93 \times 10^1$
	4	$3.41 \times 10^{-2}$	8.16	8.06	$1.48 \times 10^2$	$3.85 \times 10^2$	$1.81 \times 10^1$	$1.84 \times 10^1$
	5	$1.41 \times 10^{-2}$	$2.10 \times 10^{-1}$	$1.84 \times 10^{-1}$	$1.47 \times 10^2$	$7.00 \times 10^2$	$7.01 \times 10^2$	$7.99 \times 10^2$
	6	$2.00 \times 10^{-2}$	$2.46 \times 10^{-1}$	$2.13 \times 10^{-1}$	$5.05 \times 10^1$	$6.70 \times 10^2$	$2.05 \times 10^2$	$2.37 \times 10^2$
	7	$1.41 \times 10^{-2}$	$9.45 \times 10^{-2}$	$4.43 \times 10^{-2}$	$2.53 \times 10^1$	$1.04 \times 10^3$	$2.67 \times 10^2$	$5.70 \times 10^2$

Table 5: Nonnegative least squares results, strongly convex case, and step size fixed across  $K$ . Corresponds to Figure 4 (first part).

$t$	$K$	VPSDP	SM	PEP	VPSDP solve time (s)	$\frac{\text{PEP}}{\text{VPSDP}}$	$\frac{\text{PEP}}{\text{SM}}$
0.01	1	$6.59 \times 10^1$	$6.55 \times 10^1$	$1.88 \times 10^2$	$6.68 \times 10^1$	2.86	2.88
	2	$1.01 \times 10^1$	$1.00 \times 10^1$	$3.72 \times 10^1$	$1.49 \times 10^2$	3.68	3.71
	3	2.14	2.13	$1.30 \times 10^1$	$2.51 \times 10^2$	6.05	6.09
	4	$5.30 \times 10^{-1}$	$5.25 \times 10^{-1}$	5.67	$4.05 \times 10^2$	$1.07 \times 10^1$	$1.08 \times 10^1$
	5	$1.44 \times 10^{-1}$	$1.39 \times 10^{-1}$	2.80	$5.63 \times 10^2$	$1.94 \times 10^1$	$2.01 \times 10^1$
	6	$5.35 \times 10^{-2}$	$3.84 \times 10^{-2}$	1.49	$7.06 \times 10^2$	$2.78 \times 10^1$	$3.87 \times 10^1$
	7	$1.67 \times 10^{-2}$	$1.09 \times 10^{-2}$	$8.29 \times 10^{-1}$	$5.10 \times 10^2$	$4.96 \times 10^1$	$7.63 \times 10^1$
	8	$9.88 \times 10^{-3}$	$3.15 \times 10^{-3}$	$4.79 \times 10^{-1}$	$5.28 \times 10^2$	$4.84 \times 10^1$	$1.52 \times 10^2$
	9	$7.52 \times 10^{-3}$	$9.27 \times 10^{-4}$	$2.83 \times 10^{-1}$	$8.56 \times 10^2$	$3.76 \times 10^1$	$3.05 \times 10^2$
	10	$5.45 \times 10^{-2}$	$2.78 \times 10^{-4}$	$1.70 \times 10^{-1}$	$9.80 \times 10^2$	3.12	$6.13 \times 10^2$
0.0125	1	$1.03 \times 10^2$	$1.02 \times 10^2$	$2.94 \times 10^2$	$7.17 \times 10^1$	2.86	2.88
	2	7.19	7.14	$4.14 \times 10^1$	$1.60 \times 10^2$	5.75	5.80
	3	1.02	1.01	$1.23 \times 10^1$	$2.74 \times 10^2$	$1.21 \times 10^1$	$1.22 \times 10^1$
	4	$1.67 \times 10^{-1}$	$1.63 \times 10^{-1}$	4.77	$3.82 \times 10^2$	$2.85 \times 10^1$	$2.92 \times 10^1$
	5	$3.57 \times 10^{-2}$	$2.83 \times 10^{-2}$	2.11	$5.64 \times 10^2$	$5.93 \times 10^1$	$7.46 \times 10^1$
	6	$1.42 \times 10^{-2}$	$5.14 \times 10^{-3}$	1.01	$7.16 \times 10^2$	$7.13 \times 10^1$	$1.97 \times 10^2$
	7	$1.30 \times 10^{-2}$	$9.71 \times 10^{-4}$	$5.07 \times 10^{-1}$	$5.73 \times 10^2$	$3.90 \times 10^1$	$5.22 \times 10^2$
	8	$2.17 \times 10^{-2}$	$1.90 \times 10^{-4}$	$2.63 \times 10^{-1}$	$5.11 \times 10^2$	$1.21 \times 10^1$	$1.38 \times 10^3$
	9	$2.41 \times 10^{-2}$	$3.87 \times 10^{-5}$	$1.39 \times 10^{-1}$	$8.33 \times 10^2$	5.79	$3.60 \times 10^3$
	10	$7.59 \times 10^{-3}$	$8.17 \times 10^{-6}$	$7.51 \times 10^{-2}$	$1.01 \times 10^3$	9.90	$9.19 \times 10^3$
0.015	1	$1.48 \times 10^2$	$1.47 \times 10^2$	$4.24 \times 10^2$	$6.80 \times 10^1$	2.86	2.88
	2	5.56	5.50	$1.06 \times 10^2$	$1.60 \times 10^2$	$1.91 \times 10^1$	$1.93 \times 10^1$
	3	$3.93 \times 10^{-1}$	$3.87 \times 10^{-1}$	$2.65 \times 10^1$	$2.61 \times 10^2$	$6.74 \times 10^1$	$6.85 \times 10^1$
	4	$4.00 \times 10^{-2}$	$3.38 \times 10^{-2}$	6.62	$3.99 \times 10^2$	$1.66 \times 10^2$	$1.96 \times 10^2$
	5	$1.78 \times 10^{-2}$	$3.42 \times 10^{-3}$	1.66	$5.89 \times 10^2$	$9.32 \times 10^1$	$4.85 \times 10^2$
	6	$7.34 \times 10^{-3}$	$3.85 \times 10^{-4}$	$6.39 \times 10^{-1}$	$6.81 \times 10^2$	$8.71 \times 10^1$	$1.66 \times 10^3$
	7	$7.22 \times 10^{-3}$	$4.79 \times 10^{-5}$	$2.86 \times 10^{-1}$	$5.80 \times 10^2$	$3.96 \times 10^1$	$5.98 \times 10^3$
	8	$3.72 \times 10^{-2}$	$6.49 \times 10^{-6}$	$1.32 \times 10^{-1}$	$4.92 \times 10^2$	3.54	$2.03 \times 10^4$
	9	$2.11 \times 10^{-2}$	$9.56 \times 10^{-7}$	$6.19 \times 10^{-2}$	$8.96 \times 10^2$	2.93	$6.48 \times 10^4$
	10	$1.59 \times 10^{-2}$	$1.52 \times 10^{-7}$	$2.95 \times 10^{-2}$	$8.94 \times 10^2$	1.85	$1.94 \times 10^5$

Table 6: Nonnegative least squares results, strongly convex case, and step size fixed across  $K$ . Corresponds to Figure 4 (second part).

$t$	$K$	VPSDP	SM	PEP	VPSDP solve time (s)	$\frac{\text{PEP}}{\text{VPSDP}}$	$\frac{\text{PEP}}{\text{SM}}$
0.0167	1	$1.83 \times 10^2$	$1.82 \times 10^2$	$5.23 \times 10^2$	$7.51 \times 10^1$	2.86	2.88
	2	8.14	8.03	$2.33 \times 10^2$	$1.61 \times 10^2$	$2.86 \times 10^1$	$2.90 \times 10^1$
	3	$6.32 \times 10^{-1}$	$6.19 \times 10^{-1}$	$1.03 \times 10^2$	$2.72 \times 10^2$	$1.64 \times 10^2$	$1.67 \times 10^2$
	4	$6.29 \times 10^{-2}$	$5.17 \times 10^{-2}$	$4.59 \times 10^1$	$4.03 \times 10^2$	$7.30 \times 10^2$	$8.89 \times 10^2$
	5	$1.27 \times 10^{-2}$	$4.70 \times 10^{-3}$	$2.04 \times 10^1$	$5.64 \times 10^2$	$1.61 \times 10^3$	$4.34 \times 10^3$
	6	$8.67 \times 10^{-3}$	$4.58 \times 10^{-4}$	9.08	$7.09 \times 10^2$	$1.05 \times 10^3$	$1.98 \times 10^4$
	7	$3.06 \times 10^{-2}$	$4.77 \times 10^{-5}$	4.03	$5.34 \times 10^2$	$1.32 \times 10^2$	$8.46 \times 10^4$
	8	$8.38 \times 10^{-3}$	$5.38 \times 10^{-6}$	1.79	$5.26 \times 10^2$	$2.14 \times 10^2$	$3.33 \times 10^5$
	9	$1.05 \times 10^{-2}$	$6.71 \times 10^{-7}$	$7.97 \times 10^{-1}$	$9.83 \times 10^2$	$7.57 \times 10^1$	$1.19 \times 10^6$
	10	$1.15 \times 10^{-2}$	$9.31 \times 10^{-8}$	$3.54 \times 10^{-1}$	$9.74 \times 10^2$	$3.09 \times 10^1$	$3.80 \times 10^6$
0.0175	1	$2.02 \times 10^2$	$2.01 \times 10^2$	$5.77 \times 10^2$	$7.33 \times 10^1$	2.86	2.88
	2	$1.14 \times 10^1$	$1.13 \times 10^1$	$3.25 \times 10^2$	$1.53 \times 10^2$	$2.85 \times 10^1$	$2.88 \times 10^1$
	3	1.30	1.27	$1.83 \times 10^2$	$2.58 \times 10^2$	$1.41 \times 10^2$	$1.43 \times 10^2$
	4	$1.69 \times 10^{-1}$	$1.61 \times 10^{-1}$	$4.59 \times 10^1$	$4.30 \times 10^2$	$2.72 \times 10^2$	$2.86 \times 10^2$
	5	$3.08 \times 10^{-2}$	$2.17 \times 10^{-2}$	$5.78 \times 10^1$	$5.88 \times 10^2$	$1.88 \times 10^3$	$2.67 \times 10^3$
	6	$1.55 \times 10^{-2}$	$3.04 \times 10^{-3}$	$3.25 \times 10^1$	$1.13 \times 10^3$	$2.09 \times 10^3$	$1.07 \times 10^4$
	7	$1.00 \times 10^{-2}$	$4.47 \times 10^{-4}$	$1.83 \times 10^1$	$5.32 \times 10^2$	$1.82 \times 10^3$	$4.09 \times 10^4$
	8	$9.63 \times 10^{-3}$	$6.87 \times 10^{-5}$	$1.03 \times 10^1$	$5.23 \times 10^2$	$1.07 \times 10^3$	$1.50 \times 10^5$
	9	$3.35 \times 10^{-2}$	$1.13 \times 10^{-5}$	5.78	$9.84 \times 10^2$	$1.72 \times 10^2$	$5.10 \times 10^5$
	10	$9.90 \times 10^{-3}$	$2.03 \times 10^{-6}$	3.25	$1.15 \times 10^3$	$3.29 \times 10^2$	$1.60 \times 10^6$
0.02	1	$2.64 \times 10^2$	$2.62 \times 10^2$	$7.54 \times 10^2$	$7.63 \times 10^1$	2.86	2.88
	2	$3.34 \times 10^1$	$3.31 \times 10^1$	$7.54 \times 10^2$	$1.60 \times 10^2$	$2.26 \times 10^1$	$2.28 \times 10^1$
	3	9.24	9.11	$7.54 \times 10^2$	$2.68 \times 10^2$	$8.16 \times 10^1$	$8.27 \times 10^1$
	4	2.78	2.74	$7.54 \times 10^2$	$4.02 \times 10^2$	$2.71 \times 10^2$	$2.75 \times 10^2$
	5	$8.69 \times 10^{-1}$	$8.52 \times 10^{-1}$	$7.54 \times 10^2$	$7.29 \times 10^2$	$8.67 \times 10^2$	$8.84 \times 10^2$
	6	$2.87 \times 10^{-1}$	$2.71 \times 10^{-1}$	$7.54 \times 10^2$	$1.20 \times 10^3$	$2.62 \times 10^3$	$2.78 \times 10^3$
	7	$1.45 \times 10^{-1}$	$8.80 \times 10^{-2}$	$7.54 \times 10^2$	$5.99 \times 10^2$	$5.19 \times 10^3$	$8.56 \times 10^3$
	8	$6.48 \times 10^{-2}$	$2.92 \times 10^{-2}$	$7.54 \times 10^2$	$5.34 \times 10^2$	$1.16 \times 10^4$	$2.58 \times 10^4$
	9	$7.37 \times 10^{-2}$	$9.96 \times 10^{-3}$	$7.54 \times 10^2$	$9.48 \times 10^2$	$1.02 \times 10^4$	$7.56 \times 10^4$
	10	$6.07 \times 10^{-2}$	$3.52 \times 10^{-3}$	$7.54 \times 10^2$	$1.18 \times 10^3$	$1.24 \times 10^4$	$2.14 \times 10^5$

Table 7: Nonnegative least squares results, strongly convex case, and silver step size schedule. Corresponds to Figure 7.

Schedule	$K$	$t$	VPSDP	SM	PEP	VPSDP solve time (s)	$\frac{\text{PEP}}{\text{VPSDP}}$	$\frac{\text{PEP}}{\text{SM}}$
Strongly cvx.	1	$1.35 \times 10^{-2}$	$1.20 \times 10^2$	$1.19 \times 10^2$	$3.44 \times 10^2$	$7.17 \times 10^1$	2.86	2.88
	2	$1.77 \times 10^{-2}$	$1.04 \times 10^1$	$1.04 \times 10^1$	$8.63 \times 10^1$	$1.58 \times 10^2$	8.26	8.33
	3	$1.35 \times 10^{-2}$	$1.75 \times 10^{-1}$	$1.69 \times 10^{-1}$	$2.91 \times 10^1$	$3.05 \times 10^2$	$1.66 \times 10^2$	$1.72 \times 10^2$
	4	$2.42 \times 10^{-2}$	$8.40 \times 10^{-2}$	$7.03 \times 10^{-2}$	$1.16 \times 10^1$	$4.21 \times 10^2$	$1.39 \times 10^2$	$1.65 \times 10^2$
	5	$1.35 \times 10^{-2}$	$1.44 \times 10^{-2}$	$4.54 \times 10^{-4}$	7.29	$6.17 \times 10^2$	$5.07 \times 10^2$	$1.61 \times 10^4$
	6	$1.77 \times 10^{-2}$	$3.21 \times 10^{-2}$	$7.22 \times 10^{-5}$	1.54	$1.02 \times 10^3$	$4.81 \times 10^1$	$2.14 \times 10^4$
	7	$1.35 \times 10^{-2}$	$7.44 \times 10^{-3}$	$1.61 \times 10^{-6}$	$5.34 \times 10^{-1}$	$9.67 \times 10^2$	$7.17 \times 10^1$	$3.32 \times 10^5$

Table 8: Results for the network utility maximization experiment in Figure 9.

Init.	$K$	VPSDP	SM	PEP	VPSDP solve time (s)	$\frac{\text{PEP}}{\text{VPSDP}}$	$\frac{\text{PEP}}{\text{SM}}$
CS	1	$2.14 \times 10^2$	$2.13 \times 10^2$	$2.90 \times 10^2$	$5.45 \times 10^1$	1.35	1.36
	2	$1.49 \times 10^1$	$1.43 \times 10^1$	$1.41 \times 10^2$	$3.44 \times 10^2$	9.52	9.88
	3	7.17	7.03	$7.24 \times 10^1$	$1.17 \times 10^3$	$1.01 \times 10^1$	$1.03 \times 10^1$
	4	4.86	4.76	$3.30 \times 10^1$	$5.19 \times 10^3$	6.80	6.93
	5	3.03	2.43	$1.98 \times 10^1$	$9.88 \times 10^3$	6.55	8.17
WS	1	$1.89 \times 10^2$	$1.87 \times 10^2$	$2.44 \times 10^2$	$3.71 \times 10^1$	1.29	1.30
	2	$2.07 \times 10^1$	$2.00 \times 10^1$	$9.78 \times 10^1$	$2.72 \times 10^2$	4.72	4.90
	3	7.77	7.54	$5.64 \times 10^1$	$1.45 \times 10^3$	7.27	7.48
	4	5.27	5.08	$1.94 \times 10^1$	$4.31 \times 10^3$	3.68	3.81
	5	2.70	1.96	$1.41 \times 10^1$	$7.58 \times 10^3$	5.22	7.19
HS	1	$1.79 \times 10^2$	$1.78 \times 10^2$	$2.66 \times 10^2$	$6.42 \times 10^1$	1.48	1.50
	2	$2.04 \times 10^1$	$1.99 \times 10^1$	$1.19 \times 10^2$	$2.53 \times 10^2$	5.82	5.96
	3	9.11	8.95	$2.92 \times 10^1$	$1.37 \times 10^3$	3.21	3.27
	4	6.16	6.04	$2.83 \times 10^1$	$4.68 \times 10^3$	4.59	4.68
	5	3.22	2.67	$1.71 \times 10^1$	$8.73 \times 10^3$	5.31	6.40

Table 9: Results for the Lasso experiment in Figure 10.

Alg.	$K$	VPSDP	SM	PEP	VPSDP solve time (s)	$\frac{\text{PEP}}{\text{VPSDP}}$	$\frac{\text{PEP}}{\text{SM}}$
ISTA	1	2.24	2.22	$2.28 \times 10^2$	8.52	$1.02 \times 10^2$	$1.02 \times 10^2$
	2	1.30	1.30	$5.46 \times 10^1$	$3.14 \times 10^1$	$4.19 \times 10^1$	$4.21 \times 10^1$
	3	$9.14 \times 10^{-1}$	$9.10 \times 10^{-1}$	$2.19 \times 10^1$	$9.22 \times 10^1$	$2.40 \times 10^1$	$2.40 \times 10^1$
	4	$6.90 \times 10^{-1}$	$6.86 \times 10^{-1}$	$1.75 \times 10^1$	$1.24 \times 10^2$	$2.54 \times 10^1$	$2.55 \times 10^1$
	5	$5.46 \times 10^{-1}$	$5.43 \times 10^{-1}$	$1.57 \times 10^1$	$2.03 \times 10^2$	$2.88 \times 10^1$	$2.90 \times 10^1$
	6	$4.46 \times 10^{-1}$	$4.44 \times 10^{-1}$	$1.48 \times 10^1$	$4.09 \times 10^2$	$3.33 \times 10^1$	$3.34 \times 10^1$
	7	$3.56 \times 10^{-1}$	$3.52 \times 10^{-1}$	$1.43 \times 10^1$	$4.85 \times 10^2$	$4.02 \times 10^1$	$4.07 \times 10^1$
FISTA	1	2.24	2.22	$2.28 \times 10^2$	$1.90 \times 10^1$	$1.02 \times 10^2$	$1.02 \times 10^2$
	2	1.30	1.30	$5.46 \times 10^1$	$7.14 \times 10^1$	$4.19 \times 10^1$	$4.21 \times 10^1$
	3	1.50	1.50	$3.45 \times 10^1$	$1.85 \times 10^2$	$2.30 \times 10^1$	$2.31 \times 10^1$
	4	1.59	1.58	$4.24 \times 10^1$	$4.09 \times 10^2$	$2.67 \times 10^1$	$2.68 \times 10^1$
	5	1.55	1.54	$5.37 \times 10^1$	$8.13 \times 10^2$	$3.46 \times 10^1$	$3.48 \times 10^1$
	6	1.11	1.09	$6.82 \times 10^1$	$1.47 \times 10^3$	$6.12 \times 10^1$	$6.26 \times 10^1$
	7	$2.55 \times 10^{-1}$	$1.96 \times 10^{-1}$	$8.56 \times 10^1$	$3.15 \times 10^3$	$3.35 \times 10^2$	$4.37 \times 10^2$

Table 10: Exact verification problem results for Lasso with a 1 hour time limit with a target optimality gap of 1%. Corresponds to Figure 11.

Alg.	$K$	Best lower bound	Best upper bound	Optimality gap (%)	Gurobi solve time (s)
ISTA	1	2.24	2.26	$9.46 \times 10^{-1}$	2.96
	2	1.30	1.34	3.09	$3.60 \times 10^3$
	3	$9.14 \times 10^{-1}$	1.08	$1.81 \times 10^1$	$3.60 \times 10^3$
	4	$6.90 \times 10^{-1}$	1.50	$1.18 \times 10^2$	$3.60 \times 10^3$
	5	$5.46 \times 10^{-1}$	2.74	$4.03 \times 10^2$	$3.60 \times 10^3$
	6	$4.46 \times 10^{-1}$	1.58	$2.55 \times 10^2$	$3.60 \times 10^3$
	7	$3.54 \times 10^{-1}$	$1.08 \times 10^1$	$2.95 \times 10^3$	$3.60 \times 10^3$
FISTA	1	2.24	2.26	$9.46 \times 10^{-1}$	3.27
	2	1.30	1.34	3.10	$3.60 \times 10^3$
	3	1.50	1.66	$1.02 \times 10^1$	$3.60 \times 10^3$
	4	1.59	2.27	$4.32 \times 10^1$	$3.60 \times 10^3$
	5	1.55	2.17	$3.99 \times 10^1$	$3.60 \times 10^3$
	6	1.12	$2.89 \times 10^2$	$2.58 \times 10^4$	$3.60 \times 10^3$
	7	$1.98 \times 10^{-1}$	$6.75 \times 10^3$	$3.40 \times 10^6$	$3.60 \times 10^3$

Table 11: Results for the optimal control problem in Figure 12.

$\rho$	$K$	VPSDP	SM	PEP	VPSDP solve time (s)	$\frac{\text{PEP}}{\text{VPSDP}}$	$\frac{\text{PEP}}{\text{SM}}$
Scalar	1	$3.70 \times 10^1$	$3.68 \times 10^1$	$3.94 \times 10^2$	$4.56 \times 10^1$	$1.07 \times 10^1$	$1.07 \times 10^1$
	2	$3.54 \times 10^1$	$3.49 \times 10^1$	$7.39 \times 10^1$	$1.93 \times 10^2$	2.09	2.12
	3	$1.34 \times 10^1$	$1.33 \times 10^1$	$2.18 \times 10^1$	$5.83 \times 10^2$	1.63	1.64
	4	7.78	7.71	$1.03 \times 10^1$	$1.50 \times 10^3$	1.33	1.34
	5	5.47	5.41	6.44	$3.42 \times 10^3$	1.18	1.19
	6	3.87	3.80	4.41	$7.12 \times 10^3$	1.14	1.16
Diagonal	1	$3.70 \times 10^1$	$3.68 \times 10^1$		$4.58 \times 10^1$		
	2	$8.07 \times 10^1$	$7.99 \times 10^1$		$2.06 \times 10^2$		
	3	5.96	5.70		$6.26 \times 10^2$		
	4	$3.15 \times 10^{-1}$	$2.17 \times 10^{-1}$		$1.75 \times 10^3$		
	5	$1.16 \times 10^{-1}$	$2.70 \times 10^{-2}$		$2.92 \times 10^3$		
	6	$1.01 \times 10^{-1}$	$3.98 \times 10^{-3}$		$6.66 \times 10^3$		